REVIEW ARTICLE

Check for updates

Understanding photochemical degradation mechanisms in photoactive layer materials for organic solar cells

Jianhua Han,*[ab] Han Xu,[a] Sri Harish Kumar Paleti,[ac] Anirudh Sharma [iD][a] and Derya Baran [iD]*[a]

Over the past decades, the field of organic solar cells (OSCs) has witnessed a significant evolution in materials chemistry, which has resulted in a remarkable enhancement of device performance, achieving efficiencies of over 19%. The photoactive layer materials in OSCs play a crucial role in light absorption, charge generation, transport and stability. To facilitate the scale-up of OSCs, it is imperative to address the photostability of these electron acceptor and donor materials, as their photochemical degradation process remains a challenge during the photo-to-electric conversion. In this review, we present an overview of the development of electron acceptor and donor materials, emphasizing the crucial aspects of their chemical stability behavior that are linked to the photostability of OSCs. Throughout each section, we highlight the photochemical degradation pathways for electron acceptor and donor materials, and their link to device degradation. We also discuss the existing interdisciplinary challenges and obstacles that impede the development of photostable materials. Finally, we offer insights into strategies aimed at enhancing photochemical stability and discuss future directions for developing photostable photo-active layers, facilitating the commercialization of OSCs.

[a] *Materials Science and Engineering Program (MSE), Physical Science and Engineering Division (PSE), King Abdullah University of Science and Technology (KAUST), Thuwal 23955-6900, Kingdom of Saudi Arabia. E-mail: derya.baran@kaust.edu.sa*

[b] *Institut für Anorganische Chemie and Institute for Sustainable Chemistry & Catalysis with Boron (ICB), Julius-Maximilians-Universität Würzburg, Am Hubland, 97074 Würzburg, Germany. E-mail: jianhua.han@uni-wuerzburg.de*

[c] *Department of Chemistry and Chemical Engineering, Chalmers University of Technology, 41296, Göteborg, Sweden*

Dr. Jianhua Han completed his BSc at East China University of Science and Technology, and PhD at Dalian University of Technology under the supervision of Prof. Jinyan Wang and Xigao Jian. Following his doctoral studies, he conducted postdoctoral research with Prof. Renqiang Yang at Qingdao Institute of Bioenergy and Bioprocess Technology, and then moved to the group of Prof. Derya Baran at KAUST. In 2022, he

Jianhua Han

joined the research group of Prof. Todd B. Marder at Universität Würzburg as an Alexander von Humboldt Postdoctoral Fellow. His research interests cover synthetic chemistry and polymer materials for stable organic electronic devices.

Han Xu completed his BSc at Zhejiang University and his MSc at Northeast Normal University. Currently, he is pursuing a PhD degree under the supervision of Prof. Derya Baran at King Abdullah University of Science and Technology. His main research interests lie in developing stable organic solar cells.

Han Xu

7426 | *Chem. Soc. Rev.*, 2024, **53**, 7426–7454

This journal is © The Royal Society of Chemistry 2024

1. Introduction

Solution-processed organic solar cells (OSCs) demonstrate great potential for sustainable applications in solar power generation,[1–3] offering various advantages including light weight, mechanical flexibility, utilization of low-cost materials, "green-solvent" fabrication processes, and compatibility with the integration with large-area, flat, or curved electronic devices.[4–7] In recent years, numerous chemists have made a dedicated effort to develop electron acceptor (A) and donor (D) materials and boost device performances to over 19% efficiency.[8–14] For high-performance OSCs, the incorporation of a bulk heterojunction (BHJ) photoactive layer is crucial.[10,15,16] The BHJ layer consists of a continuous network of A and D materials, which can facilitate efficient exciton dissociation, charge generation, and transportation processes.[15,17–19] The community has witnessed several well-established models and correlations between the molecular structures of photovoltaic (PV) materials and device performance, enabling the continuous improvement of power conversion efficiencies (PCEs) over the past two decades.[10,11,20] However, the commercialization of high-performance OSCs with large-scale production and long-term stability remains a challenge in the field.[5,21,22] This challenge arises not only from cost-effectiveness concerns but also from the need for enhanced stability.[3,23–26] Therefore, to overcome these hurdles and identify stable materials, it is essential to comprehend the degradation mechanisms and establish correlations between chemical structures and device stability. Such understanding can guide material design and minimize the need for optimization *via* trial-and-error synthetic procedures that are often complex and time-consuming.[25–28]

Several factors that can influence the stability of OSCs as shown in Fig. 1 are mechanical stability (for flexible and stretchable devices), morphological stability under heat stress, solar irradiance, oxygen exposure, and moisture ingress.[24,29,30] Generally, OSC devices consist of electrodes, transport layers, and active layers. All these components in devices would suffer from environmental stress, thus impacting the overall stability of devices. It is well known that during the photo-to-electric conversion process, photovoltaic materials are inevitably subjected to illumination, either from indoor LED lighting or outdoor solar irradiance. Therefore, it is crucial to employ a D/A combination with excellent photochemical stability for the successful commercialization of OSCs. Notably, the illumination also increases the temperature of the device during operation, subsequently influencing the thermally triggered morphological stability. It is important to differentiate between photostability and heat-induced morphological stability

Dr. Sri Harish Kumar Paleti is currently pursuing his post-doctoral studies in Prof. Christian Müller's group at Chalmers University of Technology. He holds a PhD degree in Materials Science and Engineering from King Abdullah University of Science and Technology (2022) under the supervision of Prof. Derya Baran and an MSc (Hons.) in Advanced Materials and Processes from the Friedrich Alexander University Erlangen Nürnberg (2017). His research interests include the stability of organic photovoltaic devices as well as doping of organic semiconductors.

Sri Harish Kumar Paleti

Dr. Anirudh Sharma earned his PhD from Flinders University, South Australia, specializing in Nanotechnology and Surface Physics. He conducted subsequent research at the University of South Australia and the University of Bordeaux, France. Anirudh was the recipient of the Common Wealth Scientific and Industrial Research Organization (CSIRO) Future Manufacturing Flagship fellowship and has also served as a visiting researcher at the Max Planck Institute for Polymer Research. Currently, he is a research fellow at KAUST in Prof. Baran's research group OMEGALAB. His expertise lies in photovoltaics, surface physics, and the thermomechanical properties of organic semiconductors.

Anirudh Sharma

Prof. Derya Baran is an Associate Professor in Materials Science and Engineering Program at KAUST. She has completed her PhD at Friedrich Alexander University Erlangen Nürnberg in 2014, followed by a joint Helmholtz Postdoctoral fellowship between Julich Research Center and Imperial College London. Prof. Baran's research group OMEGALAB focuses on the processable semiconductors for electronic applications and materials for printed electronics.

Derya Baran

This journal is © The Royal Society of Chemistry 2024

Chem. Soc. Rev., 2024, **53**, 7426–7454 | 7427
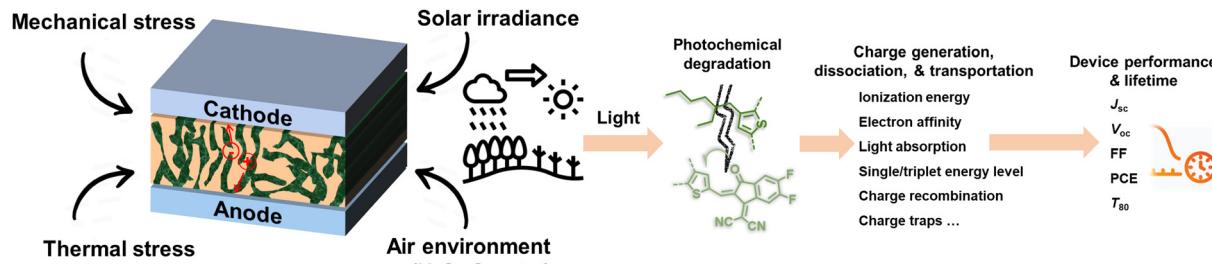
Fig. 1 Environmental factors and light-induced degradation of OSCs.

(thermal stability), following the International Summit on Organic Photovoltaic Stability (ISOS) protocol, which can be assessed through photostability measurements (such as ISOS-L) and thermostability measurements (such as ISOS-D), respectively.[31–34] Generally, heat-induced morphological stability (thermal stability) is related to physical thermodynamic behavior (mostly w/o a chemical process).[27,35] On the other hand, the photochemical stability of PV materials under illumination plays an important role in the photodegradation of OSC devices. Therefore, the photochemical degradation pathways of these materials are crucial for understanding the photodegradation mechanism of OSCs.

This review primarily focuses on the light-induced photochemical degradation of PV materials, aiming to provide guidance for synthetic chemists and the OSC community in designing stable OSCs and minimizing trial-and-error efforts. The heat-induced morphological changes (thermal stability) that occur during photostability measurements and under outdoor conditions are not covered in this review. Such thermal stability is well reviewed and can be found in the related ref. 27, 35 and 36. Generally, solar irradiance and illumination impact photostability in the following ways: (i) triggering photochemical reactions in photovoltaic molecules, (ii) causing changes in their photo-physical properties, and (iii) introducing additional traps and recombination sites, and leading to device degradation. As illustrated in Fig. 1, the photostability of OSCs is governed by the photochemical stability of these photovoltaic materials.[29,37–40] The related light-driven nm-scale morphological changes will be discussed in Section 5. It is worth mentioning that the chemical reactions between PV materials and additives can influence the device stability,[20] which is also discussed in this review (Section 5.1).

The review begins with an overview of the development of OSCs and the advancements achieved through the design of photovoltaic acceptors and donors, resulting in remarkable PCEs from 2% to over 19%.[3,10] We then provide a summary of the chemical stability of electron acceptors (Section 2), including PCBM-, PDI-, IDTBR-, ITIC-, and BTP-family acceptors as shown in Fig. 2. Then, we focus on the photochemical stability of polymer donors in Section 3, covering from polymer donors P3HT, PM6, to D18 (chemical structures detailed in Fig. 2, with corresponding abbreviations provided at the end of this review). We present the photo-degradation mechanisms of these photovoltaic acceptors and donors and discuss how light-induced chemical reactions impact molecular structural changes, leading to device degradation. Furthermore, we highlight the photochemical degradation pathways of small molecular donors, polymer acceptors and single-component materials (Section 4), which have been overlooked within the community. Finally, we discuss strategies to prevent the photochemical degradation of PV materials and the outstanding challenges associated with designing stable materials with future perspectives for OSCs as a green energy source towards commercialization. Although the molecules discussed in this review are mainly used in OSCs, the insights into the relationship between the photochemical stability of organic semiconductors and device stability will also be relevant for a range of other organic semiconductors used in organic photodetectors, organic light-emitting diodes, and integrated organic electronics for light-related device applications.

2. Chemical stability and degradation mechanisms of electron acceptors

As depicted in Fig. 2, research on OSCs has revolved around emerging acceptors, including the classic PCBM-family, ITIC-family, and the more recent BTP-family acceptors with PCEs over 19%,[3,11] along with dimer/multimer acceptors and low-cost non-fused ring acceptors.[12,14,16,65–79] It is well known that light can induce photochemical reactions, leading to the formation of photodegradation products.[24,37,38,80] Furthermore, the presence of O_2 and H_2O during illumination can facilitate these photochemical reactions and also result in the generation of additional photodegraded products.[29,81] Consequently, the photodegradation mechanisms and photochemical stability of photovoltaic materials may differ when exposed to ambient air or an inert environment. During large-scale manufacturing of OSCs, the photoactive layers will inevitably encounter ambient conditions (O_2 and H_2O), and a photostable material under ambient air can also reduce the manufacturing costs. For the long-term applications, high-quality encapsulation for OSC devices can efficiently prevent oxygen and moisture from the diffusion into the active layers, and thereby improve device lifetime.[24,82,83] Therefore, it is crucial to understand the photodegradation mechanisms of PV materials both with and without O_2/H_2O environments. Given these considerations, the following section focuses on reviewing the chemical stability

7428 | Chem. Soc. Rev., 2024, 53, 7426–7454

This journal is © The Royal Society of Chemistry 2024
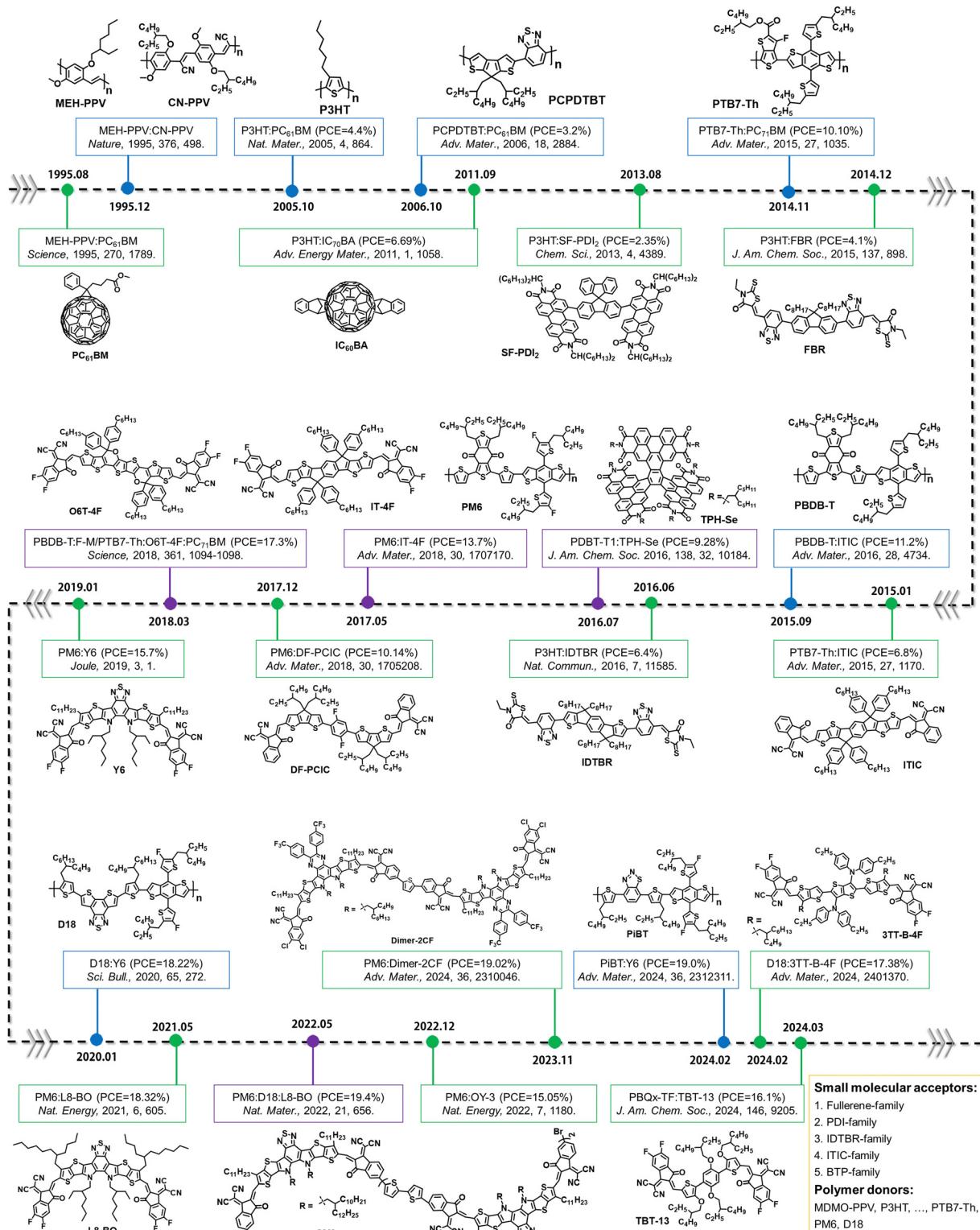
Fig. 2 Evolution of electron acceptors and polymer donors for OSCs. Since 1995, the development of OSCs has been driven by small molecular acceptors and polymer donors,[8,41,42,43,44–64] and the investigation of precise photochemical degradation pathways was primarily focused on the small molecular acceptors and polymer donors as model systems (see Sections 2 and 3). Other PV materials (small molecular donors, polymer acceptors, and single-component materials) are presented and discussed in Section 4.

This journal is © The Royal Society of Chemistry 2024

Chem. Soc. Rev., 2024, 53, 7426–7454 | 7429

and photodegradation mechanisms of the electron acceptors in ambient air and an O_2-free inert environments.

2.1 Fullerene derivatives

Electron acceptors based on fullerene derivatives, particularly $PC_{61}BM$ and $PC_{71}BM$ (the abbreviations provided at the end of this review), were widely used in the early stages of OSC research, leading to single-junction BHJ OSCs with PCEs exceeding 11%.[84,85] As illustrated in Fig. 3(a), in the presence of light and O_2, the fullerene-based derivatives are prone to undergo a photo-oxidation process, primarily affecting the fullerene cage. This photodegradation can occur even under low light conditions such as sample preparation and ambient characterization in laboratory environments.[38] During the photochemical degradation process under illumination, PCBM derivatives form various oxidative defects within the fullerene cage, such as epoxide, diol, and carbonyl structures, as confirmed experimentally through matrix-assisted laser desorption/ionization time-of-flight mass spectrometry (MALDI-TOF), ultraviolet photoelectron spectroscopy (UPS), and near-edge X-ray absorption fine structure (NEXAFS) analysis with the theoretical support of density functional theory (DFT) calculations.[38,86] As shown in Fig. 3(b) and (c), the presence of oxidized PCBM in the active layers increases energetic disorder. Li *et al.* have quantitatively correlated the fraction of oxidized fullerene with decreased electron mobility and charge lifetime.[38] The increasing number of additional trap states induced by oxidized PCBM contributes to degradation in charge carrier densities, electron transport, and recombination, leading to losses in open-circuit voltage (V_{oc}), short-circuit current (J_{sc}), and fill factor (FF) of the devices.

Besides the photochemical reactions of electron acceptors exposed to light and oxygen, Li *et al.* have demonstrated that the formation of superoxide radical ions in the active layers is another crucial factor that controls the photostability of electron acceptors.[88] The correlation is observed between the
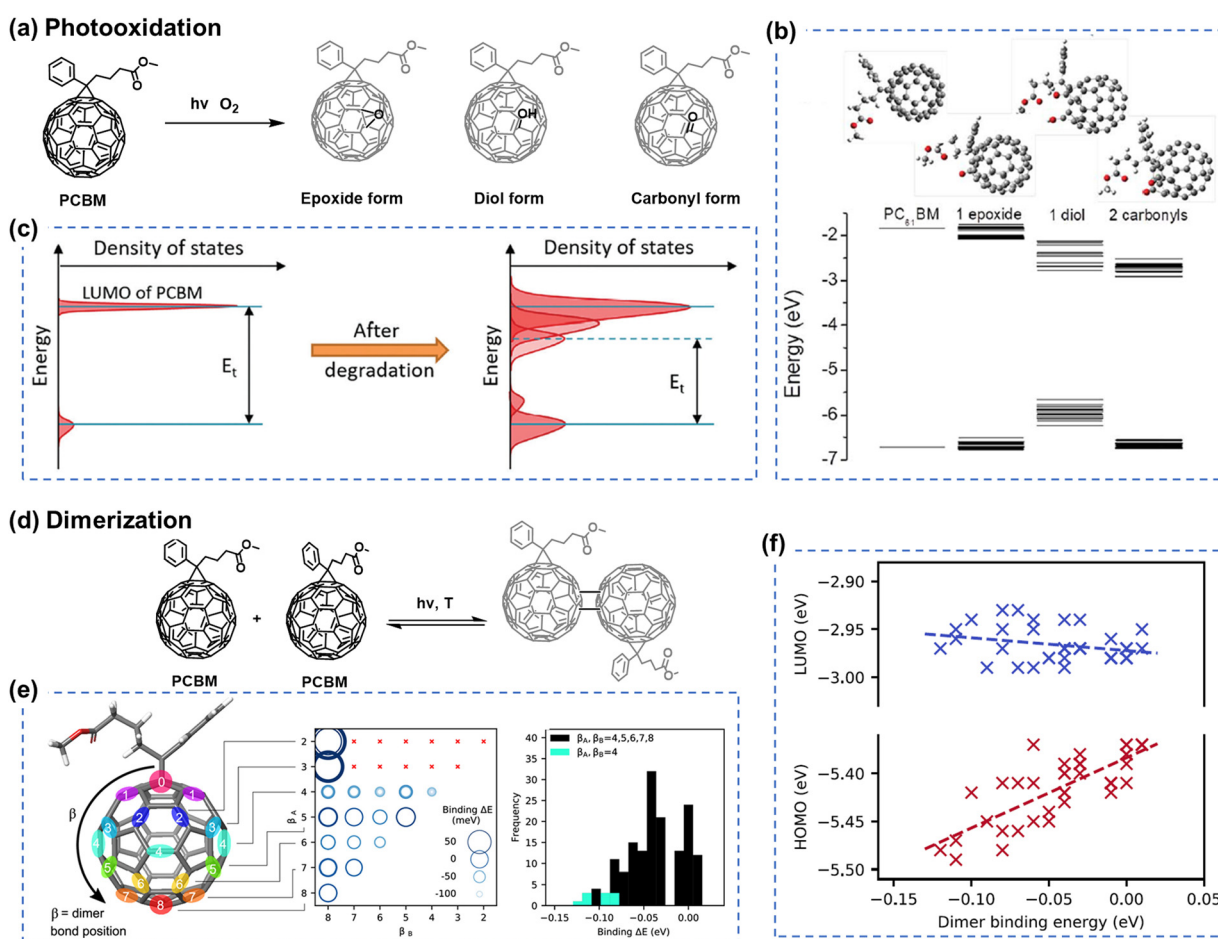

Fig. 3 (a) Photooxidation process of PCBM under combined light and oxygen stresses. (b) Energy levels of the HOMO and LUMO for the neat PCBM and various photo-oxidated PCBMs with one epoxide, one diol, or two carbonyl defects, highlighting various positions on the fullerene cage. (c) Schematic illustrating the energetic disorder induced by photodegradation products.[38] Reproduced from ref. 38 with permission from RSC Publishing, Copyright 2018. (d) Dimerization of PCBM under light and thermal stresses. (e) DFT calculations of potential PCBM dimer configurations. Reactive sites at double bonds between hexagonal faces, featuring 8 classes with equivalent distances from the PCBM tail unit. (f) Dependency of the PCBM dimer binding energy on each fullerene class presented in Fig. 3(e). These energetic disorders can induce the performance degradation in OSCs.[87] Reproduced from ref. 87 with permission from the American Chemical Society, Copyright 2019.

7430 | *Chem. Soc. Rev.*, 2024, **53**, 7426–7454

This journal is © The Royal Society of Chemistry 2024

lowest unoccupied molecular orbital (LUMO) level of electron acceptors and the resulting environmental stability of OSCs, influenced by the formation of superoxide in the blends. Consequently, electron acceptors with deeper LUMOs and suppressed oxidation processes are desired to achieve long-term stability for fullerene-based OSCs in the presence of O_2.

When transitioning to an environment without O_2, as depicted in Fig. 3(d), fullerenes tend to form dimers under illumination. Interestingly, Durrant et al. have demonstrated that fullerenes can form different types of dimers, ranging from weak to strongly bound, depending on the intensity of the illumination.[87] These distinct dimers exhibit different LUMO and highest occupied molecular orbital (HOMO) levels, as shown in Fig. 3(e) and (f). Additionally, it has been proven that this dimerization process is reversible under light and heat stress.[89] Therefore, light-induced dimerization can be considered a post-treatment process to optimize device performance, similar to thermal annealing.[90] This indicates that although thermal stability is not driven by the same mechanism as photochemical stability, such dimeric chemical structures and reversible process with light/heat stress allow the researchers to build the correlation between morphological stability and photostability in PCBM-based devices when stability tests are conducted in an inert atmosphere (in the absence of O_2 and without the formation of oxidation products).[91]

However, it is worth mentioning, in general, that the photostability of OSCs (chemical structure changes and reactions) is not directly linked to their morphological stability under thermal stress.[27] This is particularly applicable in the case of the relatively thermal stable non-fullerene acceptor (NFA) blends under room temperature, such as ITIC- and BTP-family NFAs.[36,92,93] A more detailed discussion is given in Section 5.2.

2.2 PDI derivatives

Although fullerene-based OSCs have achieved PCEs of 11%, there still exists an efficiency gap between OSCs and perovskite/Si cells that needs to be addressed for commercialization.[21,94–96] To reduce this gap, efforts are being made to develop NFAs that can overcome the limitations of fullerene derivatives, such as difficulties in chemical modification of fullerene cages, weak absorption in the visible (vis) and near-infrared (NIR) range, and variability in band gaps.[97,98] As illustrated in Fig. 2, the field of OSCs has experienced rapid advancements with the emergence of NFAs. Perylene diimide (PDI) units, as one of the NFAs, exhibit good light absorption and favorable 3D charge transport channels similar to fullerenes, such as CRP-1 (Fig. 4(a)) with the record PCEs of 11.2% in PDI derivatives so far.[64,99,100] While significant attention has been directed towards exploring the efficiency of PDI derivatives. Limited studies have investigated the chemical stability and photodegradation mechanisms of PDI-based OSCs. Min et al. conducted photostability testing (with O_2) for five different PDI-based NFAs. As presented in Fig. 4(b)–(d), both of them suffered from UV-vis absorption losses after the photooxidation process.[81] It is noteworthy that the PDI moiety itself possesses excellent thermal and photostability (w/o O_2), making
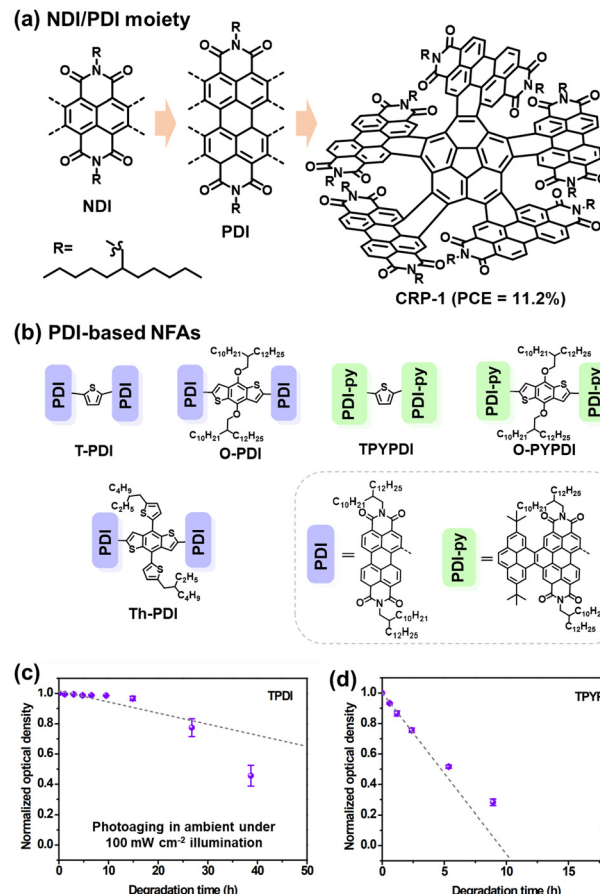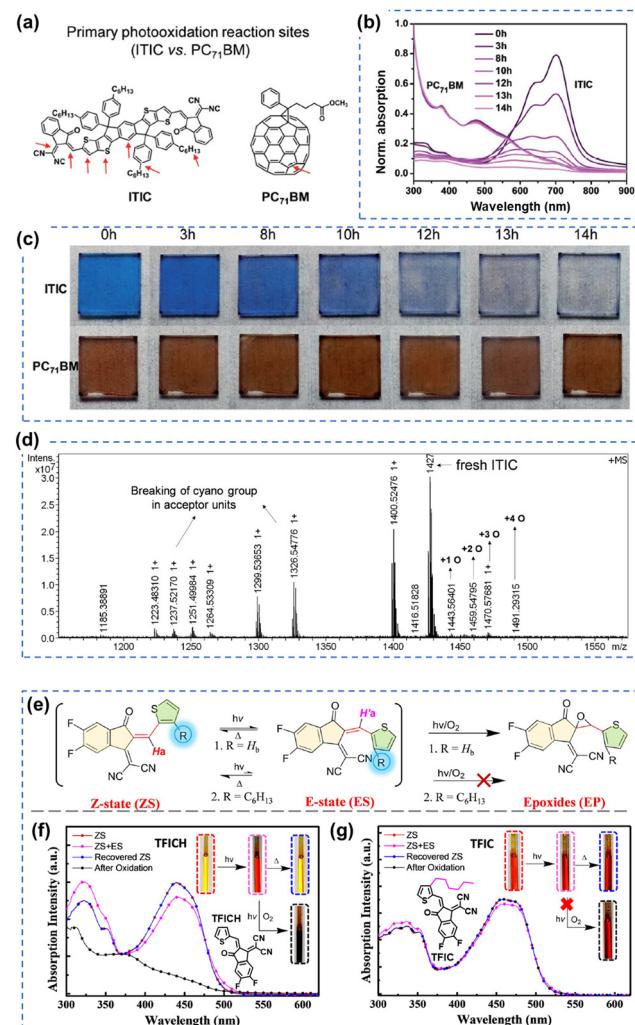

Fig. 4 (a) Chemical structures of naphthalene diimide and perylene diimide (NDI/PDI) derivatives and the PDI-based acceptor with the record PCEs obtained in binary OSCs to date.[99] (b)–(d) Chemical structures of PDI-based acceptors and their UV-vis absorption loss under illumination (photooxidation), relative to the initial maximum optical density before photoaging.[81] Reproduced from ref. 81 with permission from RSC Publishing, Copyright 2019.

it suitable for applications as lasers, filter materials, and structural components in different environments.[101,102]

In OSC research, some reports have shown that PDI derivatives can serve as stable transport layers, contributing to the achievement of highly stable OSCs.[103] Moreover, PDI moieties have demonstrated good photostability even when in contact with photo-catalyst ZnO.[104] Therefore, although the efficiency of PDI-family NFAs currently lags far behind that of ITIC- and BTP-family NFAs, PDI derivatives could still be potentially considered as a class of NFAs with promising photostability.

2.3 IDTBR and IDFBR derivatives (A–D–A type NFAs)

The acceptor–donor–acceptor (A–D–A) type small molecule acceptors have emerged as a particularly promising alternative to fullerenes and 3D-type PDIs during the past few years.[3] Notably, their capacity to consistently achieve PCEs exceeding 13% marks a significant stride in the field over fullerene counterparts since 2016.[57] The classification as A–D–A type acceptors derives from their distinctive molecular architecture:

This journal is © The Royal Society of Chemistry 2024

Chem. Soc. Rev., 2024, 53, 7426–7454 | 7431

Fig. 5 Photochemical stability (with O$_2$) of IDTBR and IDFBR-based acceptors. (a) and (b) Chemical structures of IDTBR and IDFBR. (c) Simulated Raman spectra and the assignment of Raman peaks. (d) and (e) Photodegradation behaviors of IDTBR and IDFBR were investigated by Raman spectroscopy.[106] Reproduced from ref. 106 with permission from Wiley-VCH, Copyright 2019. (f) Chemical Structures of a-IDTBTRh and l-IDTBTRh. (g) Energy barriers for the rotation modes. (h) Images of the photobleaching effect of thin films. (i) Photobleaching rates of a-IDTBTRh and l-IDTBTRh. (j) Schematic for the photooxidation process of a-IDTBTRh and l-IDTBTRh-based thin films processed from a different treatment.[107] Reproduced from ref. 107 with permission from Wiley-VCH, Copyright 2021.

a central electron-rich donor core flanked on either side by electron-deficient acceptor units.

The fluorene moiety emerged as one of the pioneering donor units in A–D–A type NFAs, chosen for its facile synthesis, ready availability, and the ease with which solubilizing chains could be incorporated to exert control over structural characteristics.[10] In 2015, Holliday *et al.* synthesized an A–D–A type NFA named IDFBR (Fig. 5), featuring an alkylated fluorene donor at its core, flanked by electron-withdrawing benzothiadiazole and 3-ethylrhodanine units in the periphery.[51] Subsequently, the substitution of the fluorene donor unit in IDFBR with an indacenodithiophene (IDT) core resulted in another notable A–D–A type acceptor known as IDTBR (Fig. 5(a)).[54] Baran *et al.* reported that the o-IDTBR, equipped with phenyl side-chains, demonstrated a PCE of 7.8% when paired with polymer donor P3HT.[18] Transitioning to EH-IDTBR, featuring branched alkyl side chains, yielded an impressive 11.1% PCE, facilitated by the use of the non-chlorinated processing solvent mesitylene without any additives.[105]

Despite the structure optimization on IDTBR-type NFAs for achieving high PCEs, the photostability of IDTBR derivatives was mainly investigated under an O$_2$ environment. As illustrated in Fig. 5(a)–(e), Kim *et al.* have systematically probed the pivotal influence of molecular structure and conformation on the photostability of IDTBR and IDFBR-based NFAs in ambient air using Raman spectroscopy.[106] This investigation entails a comparison between the planar IDTBR and the non-planar IDFBR, which exhibit structural similarities but distinct conformations. The study unveils a tripartite degradation pathway: (1) initiation of photoinduced conformational change: a phase involves the induction of photoinduced conformational changes, specifically torsional rotation related to the dihedral angles between the core and benzothiadiazole units. This conformational modulation is proposed to be instigated by noncovalent interactions with environmental moieties. (2) Subsequent photo-oxidation and fragmentation: such photo-oxidation and fragmentation processes precipitate chromophore bleaching and the formation of degradation byproducts. (3) Final chromophore bleaching: the ultimate phase culminates in complete chromophore bleaching. This comprehensive analysis underscores the pivotal role of the initial conformational transition as a decisive prerequisite for the ensuing stages of degradation.

evidenced by nuclear magnetic resonance (NMR) and MALDI-TOF results. Within these three different NFAs with fused (IT-4F, also known as ITIC-4F), semi-fused (HF-PCIC), and non-fused backbones (PTIC), non-fused PTIC demonstrates superior photostability both in solutions, films, and OSC devices. Non-fused PTIC-based OSCs even exhibit decay rates approximately 359 times slower than the fused counterpart (IT-4F), and 322 times slower than the semi-fused counterpart (HF-PCIC). This enhancement arises from the effective suppression of the photoisomerization reaction of NFAs (the structural confinement effect), occurring both at the molecular level and within thin-film states.

2.4.2 Photodegradation mechanisms of ITIC derivatives without involving an oxidation process. Under an inert atmosphere or high-quality encapsulation, the photooxidation process of PV materials can be efficiently suppressed.[24,82,83] Li *et al.* conducted a comprehensive investigation on the photostability of OSCs under a N_2 atmosphere, utilizing various NFAs, including O-IDTBR, EH-IDTBR, ITIC, and ITIC-M.[110] They found that the devices incorporating ITIC and ITIC-M still suffered from burn-in losses and long-term degradation under an inert atmosphere. As presented in Fig. 7, using *in situ* Raman measurements, they show that the photodegradation pathway in ITIC and ITIC-M is attributed to the conformational twisting between the end-group and the main backbone, along with potential bond breakage, leading to compromised device stability.

In 2021, for the first time, Perepichka *et al.* successfully isolated the photodegradation products and identified the photodegradation pathways for ITIC-family NFAs.[37] As summarized in Fig. 8(a), they demonstrated that under an inert

Fig. 8 (a) Photodegradation pathways of ITIC-4F. P1 is successfully isolated as one of the photodegradation products.[37] (b) Photodegradation pathways of IDT/IDF-based NFAs with isolated and identified photodegradation products.[80]

atmosphere (without a photooxidation process), IT-4F undergoes a photoisomerization process and then a six-electron electrocyclic reaction between the end-group unit (dicyanomethylene moiety) and the thiophene unit (in the backbone and near the dicyanomethylene moiety), followed by a 1,5-sigmatropic hydride shift. The related degradation pathway is confirmed by the isolated photodegradation product P1 with detailed structure characterization studies for the first time, such as NMR spectra, mass spectra (MS), and transition-state DFT calculations. They further examined this by mixing the photodegradation product P1 into fresh BHJ layers and correlated the photochemical stability with device stability.

Notably, in 2023, Perepichka *et al.* systematically investigated the photodegradation mechanisms of ITIC-type and other IDT-based NFAs under both an O_2 environment and an inert atmosphere.[80] First, Perepichka and co-workers showed that oxygen should selectively attack the electron-rich core rather than the electron-deficient vinylene bridge as reported by Li *et al.*[109] Under an O_2 environment, the photooxidation process, such as the formation of 1,4-enedione or ketothione, is a more favorable pathway than the 6-electron electrocyclic photoisomerization. Second, based on the clarified photodegradation pathway, they developed a series of furan-based NFAs
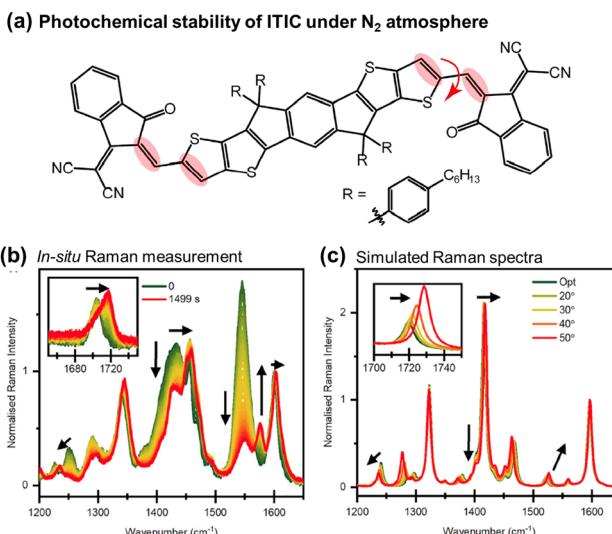
Fig. 7 (a) Chemical structure of ITIC with emphasized Raman vibrational modes during photoaging. The red arrow denotes the modified dihedral angle in Fig. 7(c). (b) *In situ* Raman spectra recorded using 514 nm laser under the N_2 atmosphere. Black arrows indicate the primary peak changes during *in situ* degradation. (c) DFT-simulated Raman spectra with increasing dihedral angles across the C–C bond in the vinylene linkage. Black arrows emphasize peak changes.[110] Reproduced from ref. 110, CC BY.

7434 | *Chem. Soc. Rev.*, 2024, **53**, 7426–7454

This journal is © The Royal Society of Chemistry 2024
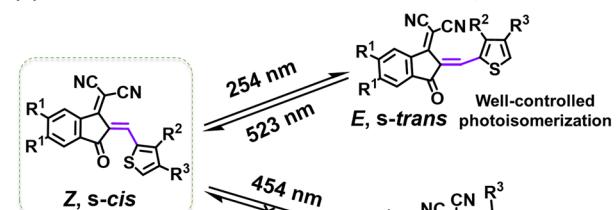
and achieved superior photovoltaic performance and photo-stability compared to thiophene-based analogs. The addition of methyl groups to the furan linkers not only reverses the conformational change but also improves intermolecular electronic coupling. Unlike the electrocyclic photoisomerization observed in many NFAs with thiophene moieties, the photo-degradation of furan-based NFAs stems from the [4+2] cycloaddition reaction of $^1O_2$ to the furan core units, resulting in the formation of a 1,4-enedione. Interestingly, the use of methyl-furan as the linker effectively mitigates both of the two degradation pathways, leading to remarkable photostability, which is proven by transition-state DFT calculations.

The complicated structures of ITIC-type NFAs (compared to fullerenes) are one of the reasons, leading to that the understanding of photostability mechanism lags far behind the development of their PCEs. Using the simplified 1,1-dicyanomethylene-3-indanon (INCN) compounds as model systems, Castellano *et al.* conducted a series of designed experiments and complementary ground- and excited-state computations.[111] As shown in Fig. 9, they offer an exhaustive examination of the photochemical characteristics of a series of INCN-based molecules, featuring variations of INCN units in (hetero-)aryl substitution, alkyl group positioning, and halogen substitution. Notably, the photoisomerization reactions are observed across all cases, facilitated by selective wavelengths of excitation spanning the ultraviolet and visible regions. In agreement with the work reported by Perepichka *et al.*,[80] Castellano and coworkers still didn't observe evidence of the photooxidation on vinylene groups as previously reported by Li *et al.*[109] Intriguingly, under irradiation at 454 nm, one of the eight INCN-based molecules exhibits both *Z/E* photoisomerization and sequential pericyclic reactions.

2.4.3 Photodegradation mechanisms of ITIC derivatives in the presence of photocatalyst ZnO. Generally, inorganic semiconductors and the metal oxides could act as catalysts to trigger chemical reactions. In the field of OSCs, ZnO has been widely used as a classic and efficient electron transport layer (ETL) since the era dominated by fullerene-based acceptors. However, in NFA-based OSCs, it is proved that ZnO has a strong photo-catalytic effect on the photodegradation process of many NFAs (w/o O_2). As shown in Fig. 10, Zhou *et al.* elucidated that a ZnO film exhibits the capability to induce the photodegradation of these high-performance NFAs (such as IT-4F, ITIC, and IEICO-4F) under UV illumination.[112] The photocatalytic effect of ZnO with UV illumination triggers the disruption of the vinyl linkage within the NFAs. This disruption, in turn, leads to the chemical decomposition of NFAs and the disappearance of intra-molecular charge transfer absorption bands. Consequently, such a photodegradation pathway contributes to a decline in device performance. In addressing this concern, Zhou *et al.* also proposed an alternative solution, suggesting the use of SnO$_2$ as ETL to enhance the photostability of inverted devices. It is noteworthy that the photocatalytic impact of ZnO in NFA-based OSCs has been consistently documented by numerous studies over the past few years.[30,113–116]

Fig. 9 (a) Photochemical behavior of 1,1-dicyanomethylene–3–indanone (INCN) based conjugated molecules. (b) ^{1}H-NMR spectra and single-crystals of the isolated compounds.[111] Reproduced from ref. 111 with permission from the American Chemical Society, Copyright 2023.

2.4.4 Summary of the photodegradation mechanisms of IDT-based NFAs and ITIC derivatives. As depicted in Fig. 11, IDT-based NFAs and ITIC derivatives undergo three distinct photo-degradation pathways: (1) oxidation process: in the presence of O$_2$, these A–D–A type NFAs generate various oxidized products. This results in energetic disorder within the BHJ layers, consequently leading to device degradation. (2) Non-oxidative process: in the absence of O$_2$, both ITIC- and IDT-based NFAs experience a photo-isomerization process and then a six-electron electrocyclic reaction between the end-group unit (dicyanomethylene moiety) and the thiophene/furan unit, followed by a 1,5-sigmatropic hydride shift. (3) Photocatalyst ZnO with UV illumination: in the presence of ZnO and UV light, the predominant pathway involves the breakage of A–D–A conjugation between the core and end-group units, leading to device degradation. These findings highlight the diverse mechanisms of photodegradation in ITIC derivatives and IDT-based NFAs and underscore the importance of understanding and mitigating these pathways for enhancing device stability.

This journal is © The Royal Society of Chemistry 2024

Chem. Soc. Rev., 2024, **53**, 7426–7454 | **7435**
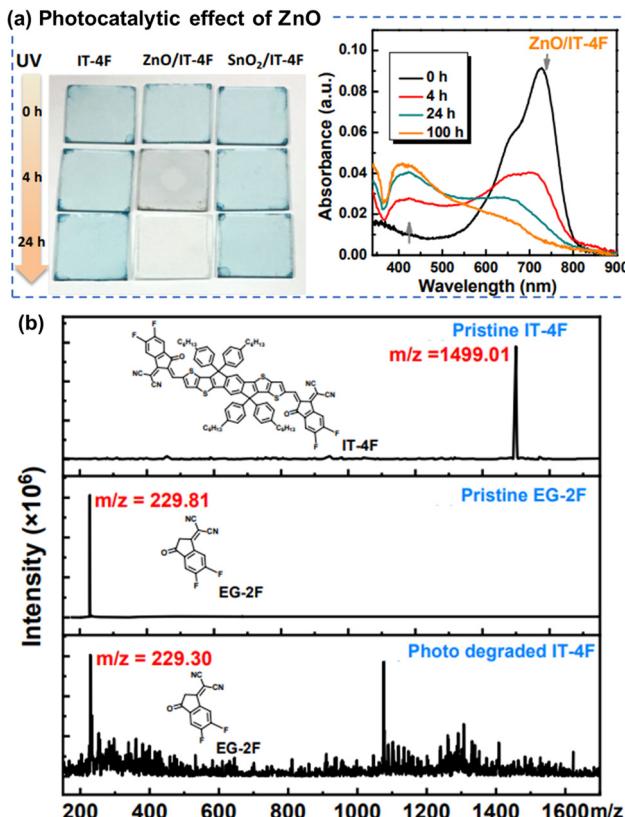
Fig. 10 (a) Photographs and UV-vis absorption spectra of the neat ITIC-4F films during photo-aging, showing the photocatalytic effect of ZnO on chemical degradation of ITIC-based NFAs. (b) MALDI-TOF spectra of the fresh and photoaged ITIC-4F-based film.[112] Reproduced from ref. 112 with permission from RSC Publishing, Copyright 2019.

2.5 BTP derivatives (A–D–A–D–A type NFAs)

In early 2019, Zou et al. developed an acceptor with central fused dithienothiophen[3.2-b]-pyrrolobenzothiadiazole core, named as BTP-4F (also known as Y6), featuring an A–D–A–D–A type backbone.[63] These BTP-series NFAs with narrow bandgap and high electron mobility enable the efficiencies of OSCs to surpass 19%.[8,60,117] Consequently, OSC research has entered a new era with BTP-NFAs as the most efficient acceptors to date. Recent reviews and perspectives have summarized and outlined the ongoing enhancements in BTP-NFAs, focusing on refining their optical and electrical properties to achieve further breakthroughs in PCEs.[3,9,11,94,96,98,118–121] In the last four years, the photostability of BTP-NFAs has predominantly been explored under controlled atmospheres (w/o O_2), while investigations into their oxidation processes remain relatively limited.[29,118] Therefore, this review aims to delve into the chemical stability and photodegradation mechanisms of BTP-based NFAs without oxidation reactions.

Recently, Kim et al. summarized the key molecular perspectives for high chemical stability of NFAs,[25] and demonstrated the increased photostability from ITIC-X (X = –Me, –H, and –F), IEICO-4F, and Y6, using in situ Raman measurements.[122] As shown in Fig. 12, owing to the existence of outer side-chains ($-C_{11}H_{23}$) in Y6 and strong intermolecular interactions in

IEICO-4F and Y6, the rotation process of vinyl groups is suppressed from ITIC-X (X = –Me, –H, and –F), IEICO-4F, to Y6, leading to the improved photostability.

Similar to ITIC derivatives, BTP-NFAs also suffered from the conjugation breakage from the vinyl linkage between the end groups and core units. As shown in Fig. 13(a), Wang et al. showed the loss of end-groups and the formation of ketone groups in BTP-NFAs (contacting with ZnO) as the main photodegradation products using MALDI-TOF spectra.[123] Loo et al. demonstrated the loss of end-groups in BTP-NFAs after the photoaging process when devices used C_{60}-SAM (self-assembled monolayer) coated ZnO as the transport layer, while the photodegradation products are end-capped with methyl groups, identified by MALDI-TOF spectra (Fig. 13(b)).[39]

The rotation of vinyl groups in A–D–A type NFAs is the initial process that induced the photodegradation of NFAs, which is proved by the isolated photodegradation products in ITIC-NFAs.[37,80,111] Although the existence of out-side-chains in BTP-NFAs can suppress such rotation modes, the flexible vinyl groups are still able to rotate under illumination. As shown in Fig. 14, Jen et al. synthesized a series of BTP-NFAs with local-isomerized conjugated side-groups, and proved the isomerization on their geometries and torsion angles can module the photostability of OSC devices, which also behaves differently from their thermal stability.[124,125]
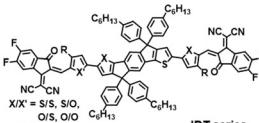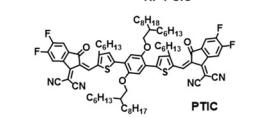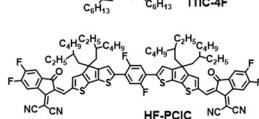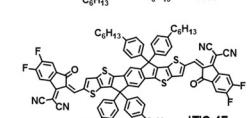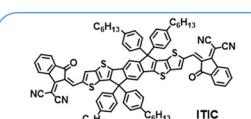
Baran et al. utilized six different NFAs with Cl/F-endgroups and side-chains as a platform to study how the molecular structures of BTP-NFAs affect the photostability and outdoor stability of OSC devices.[83] As summarized in Fig. 15, the increased energy barrier for the rotation of vinyl groups can suppress the photodegradation process of NFAs at the molecular level (steric hindrance from side-chains), and the high quadrupole moments in NFAs (fluorinated end-groups) can further prevent the rotation of vinyl groups in the solid states, which is consistent with the work reported by Kim et al.[122] The observed photostability trend among Y6, BTP-eC9, and BTP-BO-4Cl (PEDOT:PSS-based devices, Fig. 15(b)) is also consistent with the one reported by Yu et al.[126] These results show that preventing the rotation of vinyl groups is not only the key in ITIC-NFAs, but also important in BTP-NFAs, which is also reported by Du et al.[127] This is because vinyl groups exhibit high isomerization reactivity under thermal and light stress, which has been recognized since the discovery of polyacetylene film (Nobel lecture).[128] Locking the vinyl groups by rational chemical design has been proven as an effective strategy for improving the photostability of ITIC-based NFAs.[108,129] Therefore, this would also be a promising avenue for achieving photostable BTP-type NFAs.[130]

3. Chemical stability and degradation mechanisms of polymer donors

The limited diffusion length of excitons presents a challenge in achieving effective exciton separation upon generation and
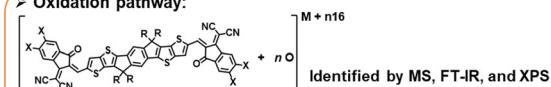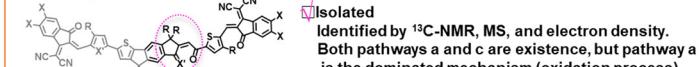
7436 | Chem. Soc. Rev., 2024, 53, 7426–7454

This journal is © The Royal Society of Chemistry 2024
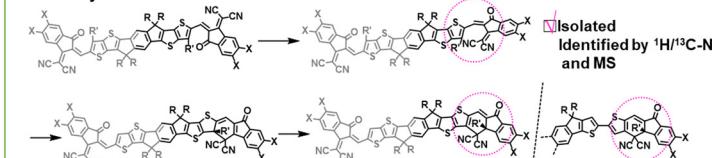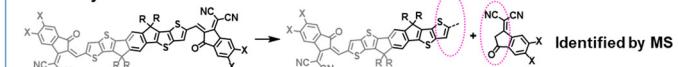
Fig. 11 Summary of the photochemical degradation pathways and photodegradation mechanisms for ITIC- and IDT-based NFAs.
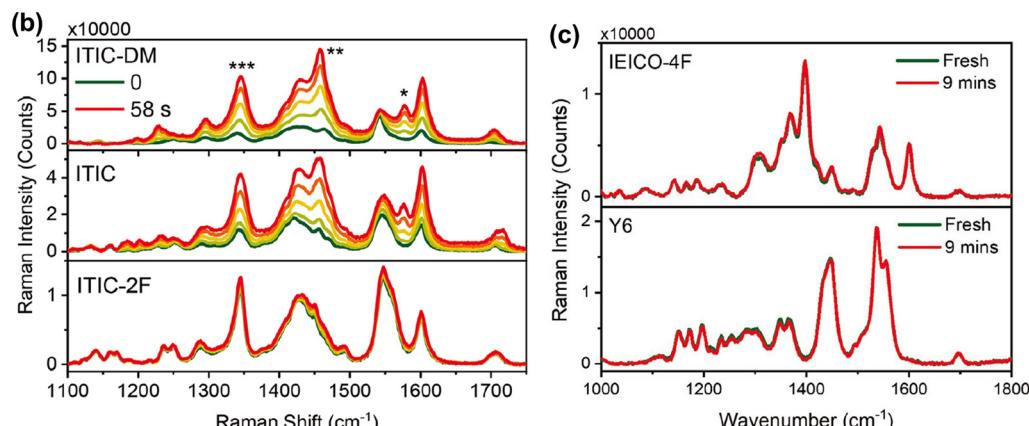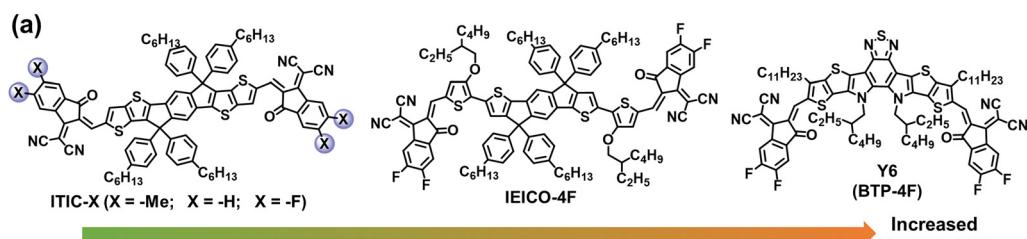
Fig. 12 (a) Chemical structures of ITIC-Me, ITIC-H, ITIC-F, IEICO-4F, and BTP-4F (also known as Y6) with increased photostability. (b) *In situ* Raman spectra (514 nm laser) of the neat ITIC-NFA films. (c) *In situ* Raman spectra (633 nm laser degradation before and after 9 min) of the IEICO-4F and Y6 neat films.[122] Reproduced from ref. 122, CC BY.

recombination in most organic semiconductors.[131] To address this, a prevailing strategy involves the nanoscale blending of electron acceptor and donor components, forming a BHJ

blend.[132] This BHJ morphological approach remains a cornerstone in the realm of OSC research.[3] Therefore, despite the photostability of electron acceptors discussed in Section 2, the

This journal is © The Royal Society of Chemistry 2024

Chem. Soc. Rev., 2024, 53, 7426–7454 | 7437
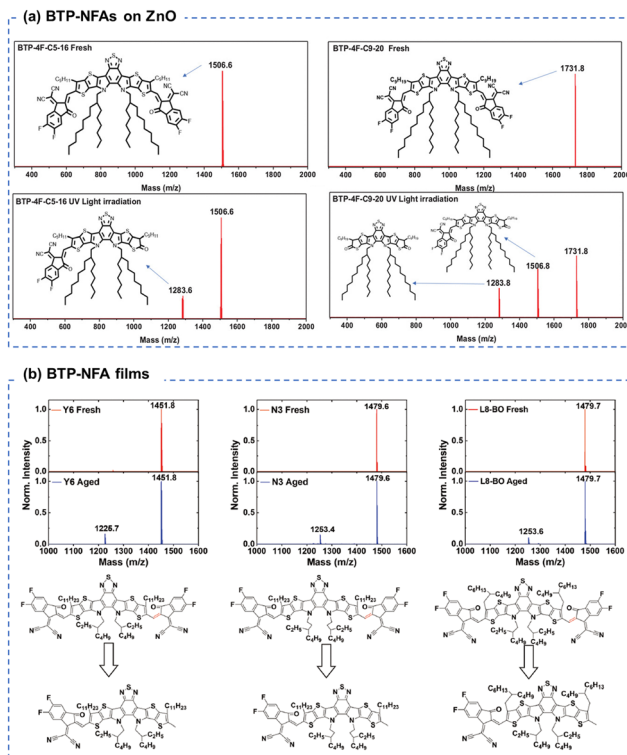
Fig. 13 (a) MALDIT-TOF spectra of the BTP-based NFA films before and after photo-aging with ZnO layers.[123] Reproduced from ref. 123 with permission from Wiley-VCH, Copyright 2022. (b) MALDIT-TOF spectra of the BTP-based NFA films before and after photo-aging.[39] Reproduced from ref. 39 with permission from Wiley-VCH, Copyright 2023.

Fig. 14 (a) Chemical structures of BTP-based NFAs with locally isomerized conjugated side-groups. (b) Storage (R.T.) and thermal stability (65 °C) of their normal-structure devices. (c) Photostability (maximum-power-point tracking, 65 °C) of the corresponding inverted devices.[124] Reproduced from ref. 124 with permission from the American Chemical Society, Copyright 2023.

photostability of polymer donors stands as another critical factor governing device stability.

Fig. 16 delineates two primary categories of polymer donors so far: D-type and D–A type. Low-cost P3HT and other D-type polymers exhibit relatively wide band gaps. To further mitigate this, the strategy of D–A hybridization has been extensively employed, integrating alternating D and A segments along the polymer backbone. This integration fosters molecular orbital mixing between D and A units, engendering a set of hybridized molecular orbitals with an effective band gap smaller than that of D-type polymer donors.[131] Consequently, D–A polymers have dominated OSC research over the past 10 years, and allow for precise control over bandgaps and energy levels *via* meticulous monomer selection.[133] This progress has led to the development of various D–A polymer donors, including PTB7-Th, PM6, D18, and PTQ10.[3,134,135]

In the following section, we will comprehensively summarize the photodegradation mechanisms of both D-type and D–A-type polymer donors, encompassing scenarios involving and excluding oxidation processes. The photostability for small molecular donors, polymer acceptors, and single-component materials will be discussed in Section 4.

3.1 Photodegradation mechanisms of polymer donors involving an oxidation proces

This section focuses on delineating the photochemical degradation pathways for polymer donors, primarily emphasizing the oxidative processes. Among these donors, P3HT, as a star polymer, remains a subject of active investigation within the community owing to its cost-effectiveness in comparison to other D–A-type polymer donors. Over the last two decades, extensive research has elucidated the photodegradation pathways of P3HT as summarized in Fig. 17. Under illumination in an oxygen environment, P3HT undergoes diverse photodegradation pathways, including H-abstraction, β-scission, cage reactions, and oxidation. These reactions generate various photodegradation products, which were identified through MS, FT-IR, and Raman spectra analyses. Consequently, the material experiences conjugation loss, alterations in HOMO/LUMO levels, and a decline in UV-vis-NIR absorbance, impacting its inherent photophysical properties and consequently leading to device degradation.[136–141]

Generally, D–A-type polymer donors share the following design concept: conjugated backbones serve as charge transport channels, and alkyl side-chains contribute to their favorable solution processability. The conjugated backbones of these polymers are susceptible to oxidation and ring-opening reactions under illumination in the presence of oxygen. The

7438 | *Chem. Soc. Rev.*, 2024, **53**, 7426–7454

This journal is © The Royal Society of Chemistry 2024
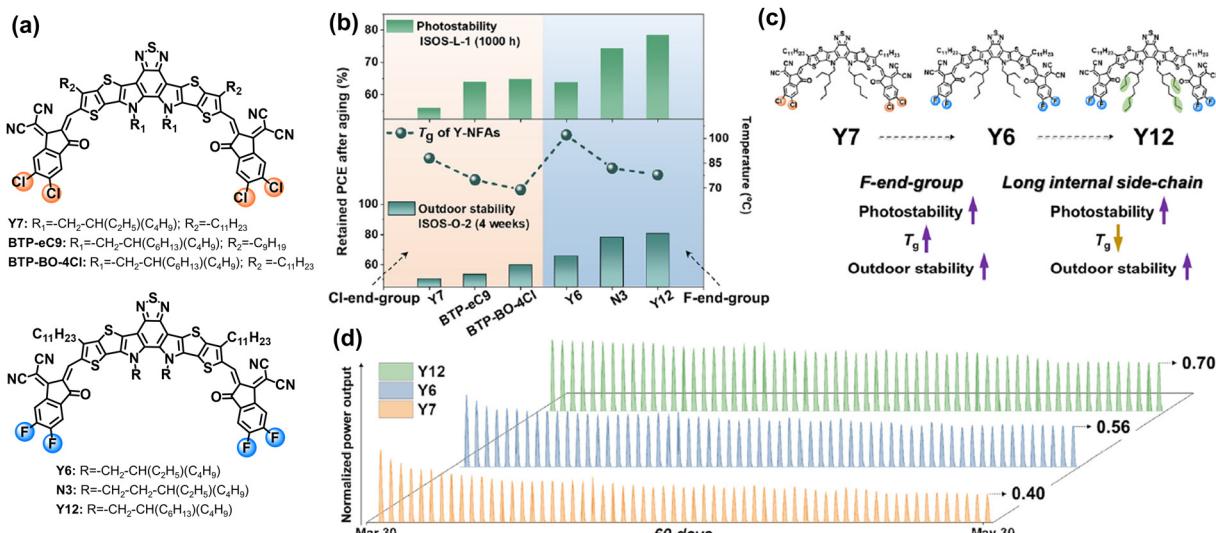
Fig. 15 (a) Chemical structures of Cl- and F-endgroup-based BTP-NFAs with different side-chains. (b) Photostability and outdoor stability of the NFA-based devices. (c) Molecular engineering on improving photostability and outdoor stability of the devices. (d) 60-day outdoor operation of the Y7-, Y6-, and Y12-based devices under hot and sunny Saudi climates.[83] Reproduced from ref. 83 with permission from Elsevier Publishing, Copyright 2023.
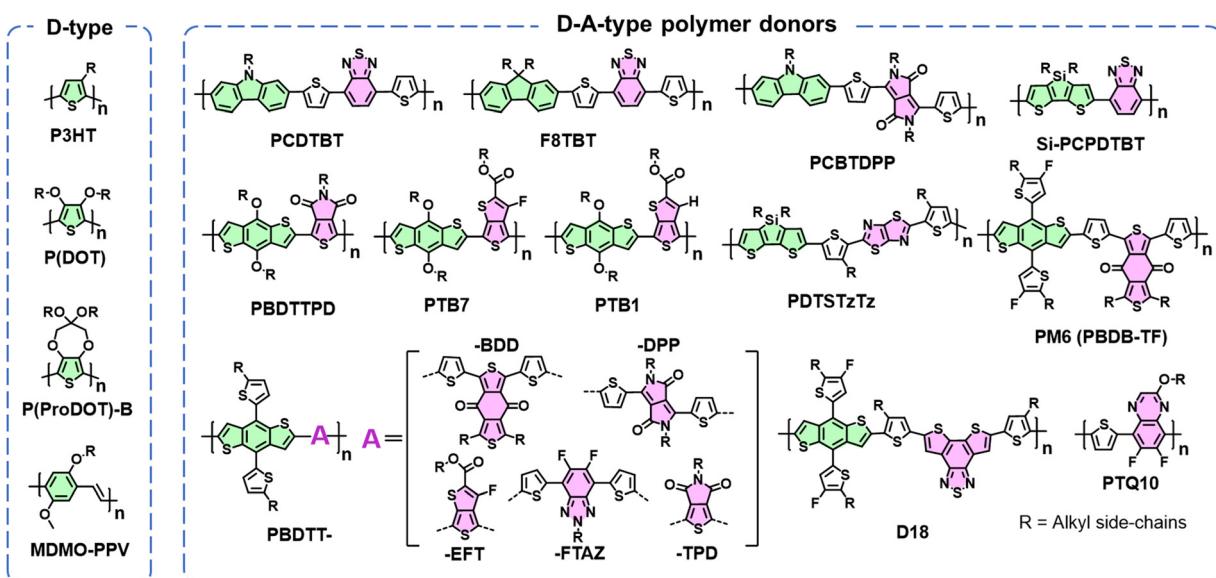
Fig. 16 Chemical structures of D-type and D−A-type polymer donors used in OSCs.

side-chains suffered from H-abstraction and scission reactions. While exploring D–A-type polymer donors, Troshin *et al.* investigated photooxidation across 16 conjugated polymers using electron spin resonance (ESR) spectroscopy. They observed that even trace amounts of oxygen (as low as 900 ppm) can facilitate and trigger photooxidation in all studied polymers. Notably, polymers with lower-lying HOMO energy levels, reflecting higher oxidation potentials, demonstrated better resistance to photooxidation. This emphasizes the role of energy levels in determining the polymer susceptibility to oxidation under light.[143]

Despite the oxidation sites on polymer backbones, the alkyl side-chains are proved to be weak links in polymer donors, along the photochemical degradation pathways, such as H-abstraction and β-scission. Tournebize *et al.* have highlighted the significance of side-chain degradation behaviors in polymer donors, positing them as a hindrance to the commercial viability of these materials.[144,145]

Recently, Ratcliff *et al.* investigated the ambient-induced photodegradation pathways of five donor polymers, featuring the same alkyl thienyl-substituted-benzodithiophene (BDTT also known as BDT) unit but with different A units.[146] Through

This journal is © The Royal Society of Chemistry 2024

Chem. Soc. Rev., 2024, **53**, 7426–7454 | **7439**
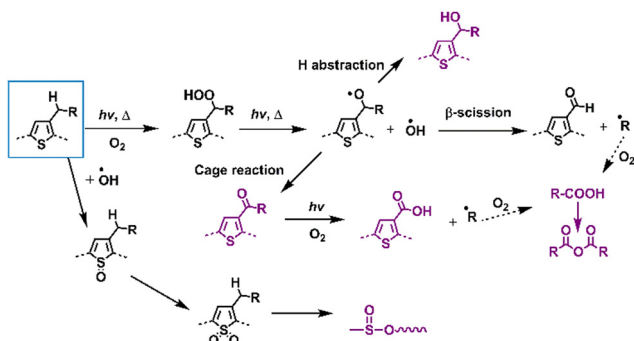
Fig. 17 Photodegradation mechanisms (with O_2) of classic D-type polymer donors – poly(thiophene) derivatives.[136–139,141,142]

controlled photobleaching in air and simultaneous absorptance monitoring, as shown in Fig. 18, they identified three different pathways. By tracking the photoaging process with XPS, they assessed near-surface chemical changes, particularly oxygen additions to sulfur and nitrogen on the BDTT or distinct A units. The results show that alkyl chain oxygen addition typically acted as the initial site of attack, followed by direct oxidation on the sulfur atom in the conjugated backbone.

In Fig. 19, the proposed photodegradation products for five classic D–A polymers were established through XPS analysis. Ratcliff *et al.* revealed that sulfur oxidation typically

Fig. 18 Photodegradation mechanisms (with O_2) and reaction pathways for the classic donor and acceptor block units in D–A type polymer donors.[144,146]

commenced after the saturation of alkyl chain oxygenation.[146] Notably, this result aligns with the findings of Manceau *et al.*,[136] indicating that direct sulfur oxidation is initiated by hydroxy radicals generated from alkyl chain oxygenation, serving as the key step. Meanwhile, ring opening reactions of thiophene/furan rings in NFAs (Fig. 8(b) and the pathway *a* in Fig. 10) and PBDTT-EFT (also known as PTB7-Th in Fig. 19) are induced by Diels–Alder addition of singlet oxygen.[80,136,146] The photochemical degradation mechanism illustrated in Fig. 19 can extend beyond D–A polymer architectures, proving relevant for a wider range of organic semiconductors. This significance also arises from the common structural template shared by most polymer donors, featuring alkyl chains on a conjugated backbone, which is consistent with the degradation pathways reported by Tournebize *et al.*[144,145] As alkyl side-chains in polymer donors are essential for ensuring the solution-processability, this contradictory behavior still presents a considerable challenge in developing stable OSCs when the device operates under an O_2 environment.

3.2 Photodegradation mechanisms of polymer donors without involving an oxidation process

With the help of high-quality encapsulation, OSC can operate with the exclusion of ambient air and prevent the ingress of oxygen and water into the BHJ layers.[82,83] Therefore, understanding the photodegradation mechanisms of polymer donors without involving an oxidation process is also important for the commercialization of OSCs. Taking P3HT as an example, researchers have shown that H-abstraction and β-scission are two main degradation pathways followed by radical recombination with the formation of cross-linking products.[137] Such cross-linking reactions can be observed in a wide range of D–A polymers when exposed to light (without O_2).[40,147] In 2019, Troshin *et al.* discovered a commonality by investigating a library of over 20 conjugated polymers and diverse structural small molecules, showing that all these materials readily undergo light-induced crosslinking. They proposed that this phenomenon likely involves light-driven [2+2] cycloaddition and radical addition photochemical reactions.[40] Recently, Troshin *et al.* found that such photodegradation pathways come from side-chain breakage.[147]

In 2022, Reynolds *et al.* conducted a comprehensive study on the photostability of D-type polymer donors under oxygen-free conditions, comprising a family of dialkoxy-functionalized thiophene polymers.[148] Employing UV-vis-NIR spectroscopy, XPS, gel permeation chromatography (GPC), NMR, and cyclic voltammetry (CV) measurements, they explored the photochemical degradation pathways, such as crosslinking, chain scission, and chemical alterations affecting the conjugated backbones (Fig. 20). The findings highlighted that crosslinking through alkyl side chains emerged as the primary degradation pathway under oxygen-free conditions. Based on these insights, they suggested promising strategies to enhance photostability in conjugated polymers, including moving away from tertiary carbon branching to either quaternary carbon branching or linear counterpart (without branching points) in side-chains, or shifting the side-chain branching point further from the main

7440 | *Chem. Soc. Rev.*, 2024, **53**, 7426–7454

This journal is © The Royal Society of Chemistry 2024

(1) PBDTT-DPP

(2) PBDTT-FTAZ

(3) PBDTT-BDD (PBDB-T)

(4) PBDTT-EFT (PTB7-Th/PCE10)

(5) PBDTT-TPD

Fig. 19 Photodegradation products (with O_2) of five different D–A type polymer donors.[146]

Fig. 20 Photodegradation mechanism (without O_2) for polymer donors: identified side-chain cross-linking pathways.[144,145,148]

and contribution of polymer donors and NFAs to the photo-degradation effect in state-of-the-art OSCs.

Gillett *et al.* investigated the photodegradation effect of PM6 and Y6 on the device stability (ZnO-based devices w/o UV, aging under white LED and in air). They investigated the photostability of three classic donor polymers – PM6, D18, and PTQ10 when paired with Y6. Upon subjecting PM6 and D18 to light exposure in ambient air, they observed a notable increase in the conversion of singlet excitons into trapped interchain polaron pairs within a timeframe of less than 100 fs. This phenomenon surpassed electron transfer to Y6, leading to a considerable reduction in the overall charge generation yield. As shown in Fig. 21, using *in situ* Raman measurements, they found that a twisting tendency within the BDT-thiophene motif, shared by PM6 and D18, is the main reason. As such, compared to Y6, the polymer donors (PM6 and D18) emerge as a weak link impacting overall OSC stability.[29] Loo *et al.* also investigated the photodegradation effect of PM6 and Y6 on the device stability (C_{60}-SAM/ZnO-based devices, aging under AM 1.5G illumination in an N_2 atmosphere).[39] They found that photochemically, PM6 is relatively stable after photo-aging for 200 h. In contrast, photochemical decomposition of Y-NFAs is responsible for the degradation of high-efficiency OSCs.

To unravel the photo-degradation mechanism within PM6:Y6-based OSCs, Yu *et al.* employed various device fabrication methods and photoaging procedures, strategically isolating the individual contributions of PM6 and Y6.[126] As depicted in Fig. 22, the comparison between devices exposed solely to the donor PM6, solely to the acceptor Y6, and those exposed as a blend strongly suggests that the degradation of PM6 predominantly governs the photodegradation process in PM6:Y6-based devices. This research presents a novel approach to investigating limitations hampering device photostability, highlighting the pivotal role of enhancing the photostability of polymer donors as a straightforward solution to improving overall device stability. Interestingly, this finding aligns with conclusions drawn from studies on perovskite-organic tandem solar cells as reported by Riedl *et al.*[149]

backbone. These modifications not only hold promises for improving the photostability of D-type polymers but also would be informative for achieving photostable D–A-type polymer donors used in OSCs.

3.3 The role of photodegradation of polymer donors in the state-of-the-art NFA OSCs

As summarized in the last two sections, it is well-known both polymer donors and electron acceptors are subjected to photo-degradation. Therefore, it is important to understand the role

4. Photochemical stability of small molecular donors, polymer acceptors, and single component materials

Given the performance of BHJ-type OSCs leading the development in this field,[2,3,21,25,117,118] extensive investigations have
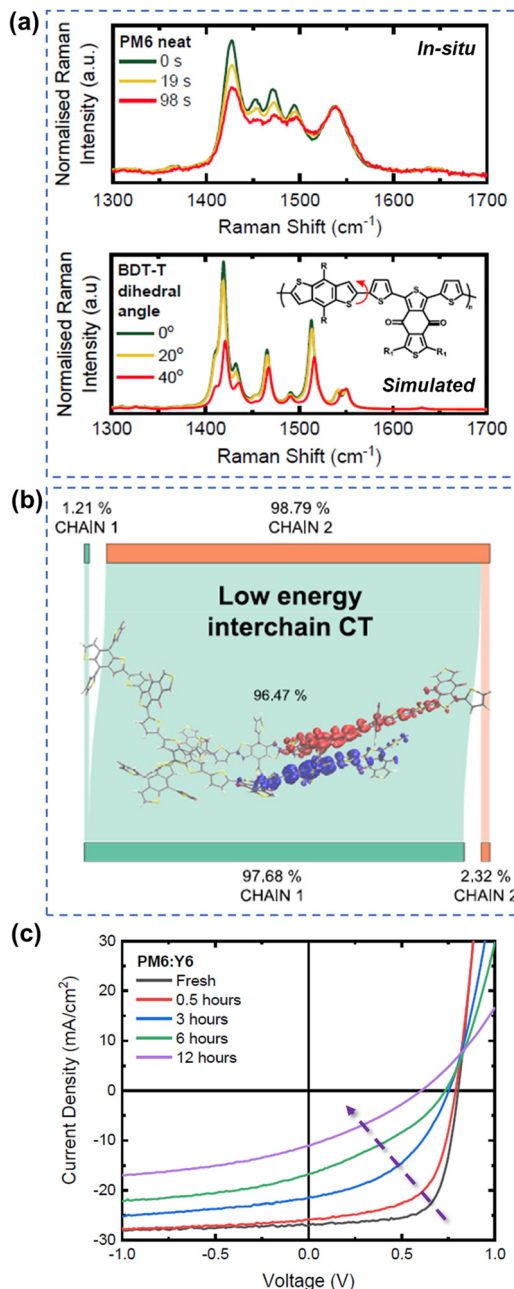
Fig. 21 (a) *In situ* Raman measurements and simulated Raman spectra for understanding photodegradation (with O₂) of PM6. (b) Structure twisting effect of PM6 induced low energy interchain charge transfer states. (c) *J–V* curves of PM6:Y6-based devices during the photoaging process (with O₂).[29] Reproduced from ref. 29, CC BY.

Fig. 22 (a) and (b) Device fabrication process for understanding the role of photodegradation (without O₂) of PM6 and Y6 in OSCs. (c) *J–V* curves of PM6:Y6-based devices using different device fabrication and photoaging processes (without O₂).[126] Reproduced from ref. 126 with permission from RSC Publishing, Copyright 2021.

centered around small molecular acceptors and polymer donors, serving as models to unravel the photodegradation mechanisms of PV materials. However, as summarized in Fig. 23, there still exist other PV materials, including small molecular donors, polymer acceptors, and single-component materials.

All small-molecular OSCs, consisting of both small molecular donors (Fig. 24(a)) and acceptors, offer distinct advantages such as well-defined chemical structures, minimal batch-to-batch variations, straightforward synthesis and purification methods, and easily adaptable properties. The development of small-molecule donors and NFAs has boosted PCEs of the devices exceeding 18%, rivalling those of their polymer-based counterparts.[150–164] The recently reported all-small-molecule ternary solar cells have delivered PCEs of 18.1% with promising operational stability.[160] Despite the reported photo-stability data of all-small-molecule-based devices,[160,165,166] the precise photochemical degradation pathways for these small molecular donors remain unclear.

A similar scenario applies to all-polymer solar cells, comprising polymer donors and polymer acceptors, where their efficiency has increased by over 18%.[167–172] In the molecular architectures of polymer acceptors depicted in Fig. 24(b), the primary advantage of all-polymer solar cells is their enhanced thermal stability in comparison to other OSCs comprising small molecular PV materials. The related thermal degradation mechanisms have been elucidated, revealing that polymerized acceptors tend to display low thermal diffusion coefficients and maintain stable morphology under thermal stress.[167] Many researchers have also conducted the photostability measurements on these devices.[173–177] However, little attention has been given to investigating the precise photochemical degradation pathways for these polymer acceptors. Unlike small molecular acceptors (fullerenes and ITIC-/BTP-NFAs as discussed in

7442 | *Chem. Soc. Rev.*, 2024, **53**, 7426–7454

This journal is © The Royal Society of Chemistry 2024

(a) Widely investigated photochemical degradation

Small molecular acceptors
(section 2)

Polymer donors
(section 3)

(b) Unraveled photochemical degradation pathways

Small molecular donors

Polymer acceptors

Single-component photovoltaic materials

Polymer (side-chain model)

Polymer (backbone model)

Molecular dyads

Homojunction molecules

Acceptor   Donor   Conjugation breakers

Fig. 23 Schematic diagrams of the photovoltaic materials: (a) widely investigated photochemical degradation mechanism for small molecular acceptors and polymer donors, and (b) limited studies on photochemical pathways for the other PV materials.

Section 2), analysing the photochemical reactions of polymers and isolating photodegraded polymeric products are challenging due to limited characterization methods and the intrinsic complexity of polymers. To achieve photostable all-polymer solar cells, a deeper understanding of the photochemical degradation pathways of polymer acceptors is imperative and significant for ensuring their photostability and minimizing trial-and-error efforts.

In addition to BHJ-type active layers comprising electron donor and acceptor materials, PV materials based on covalently linked electron donors and acceptors (referred to as "single-component materials") have also been developed as photoactive layers in OSCs for the past two decades.[72,178–193] As depicted in Fig. 24(c), recent advancements in single-component material OPVs have marked a significant stride towards achieving competitive PCEs exceeding 14%.[192] The advantages of single-component materials over other donor and acceptor materials in BHJ blends include the simplification of device fabrication process and the covalently stabilized D–A units, which facilitate thermally stable morphology and excellent device stability.[193] Researchers have also presented photostability results on single-component material OPVs, indicating promising device performance even under harsh environmental conditions such as high temperature and

continuous illumination.[179,181,184–186,188,189,191,194] However, the understanding of photochemical degradation mechanisms in these systems remains unexplored. Questions persist regarding whether the pendent acceptor units would follow the same photochemical degradation pathway as discussed in Section 2, or if the donor units undergo oxidation under illumination in the presence of O_2, and how the molecular structures of single-component materials influence the reaction rates of photochemical degradation pathways.

As summarized from Sections 2–4, current investigations into photodegradation mechanisms and photochemical degradation pathways predominantly focus on small molecular acceptors and polymer donors. Rather than solely reporting photostability results, comprehending the photodegradation pathways can effectively bridge the gap between molecular design efforts within the chemistry community and the ultimate stability performance within the device community. This understanding can help avoid reliance on trial-and-error approaches for materials design and device engineering towards enhancing overall device stability in PV technology development.

5. Chemical reactions involving additives and chemical stability of photovoltaic materials with light-driven morphological changes

Over the past decades, the exploration of photochemical pathways in OSCs has predominantly centred around small molecular acceptors and polymer donors as discussed in the above Sections 2 and 3. Furthermore, there are still other factors related to the photostability of OSCs, which will be discussed in the following sections.

5.1 The side reactions between PV materials and additives

The intrinsic photochemical stability of PV molecules holds significant importance in their photostability, and it is also essential to note the existence of side reactions between PV materials and additives. For instance, in the case of the classic additive 1,8-di-iodooctane (DIO), Jacobs et al. discovered that residual DIO can persist within the BHJ layers after the device fabrication and related post-treatment process.[195] Specifically, the weak C–I bond in DIO exhibits susceptibility to dissociation with the formation of radicals upon exposure to illumination. As depicted in Fig. 25, Brabec et al. demonstrated the capacity for both PCBM and ITIC to engage in radical reactions with DIO, forming adducts, a finding confirmed through high-performance liquid chromatography–mass spectrometry (HPLC-MS) analysis.[196] This photochemical reaction further accelerates the photodegradation process in OSCs. Meanwhile, other research groups have also reported on this similar additive-accelerated photodegradation process in OSCs.[197–199]

In addition to DIO, amine-containing materials, such as polyethylenimine (PEI) and ethoxylated PEI (PEIE), are also

This journal is © The Royal Society of Chemistry 2024

Chem. Soc. Rev., 2024, 53, 7426–7454 | 7443
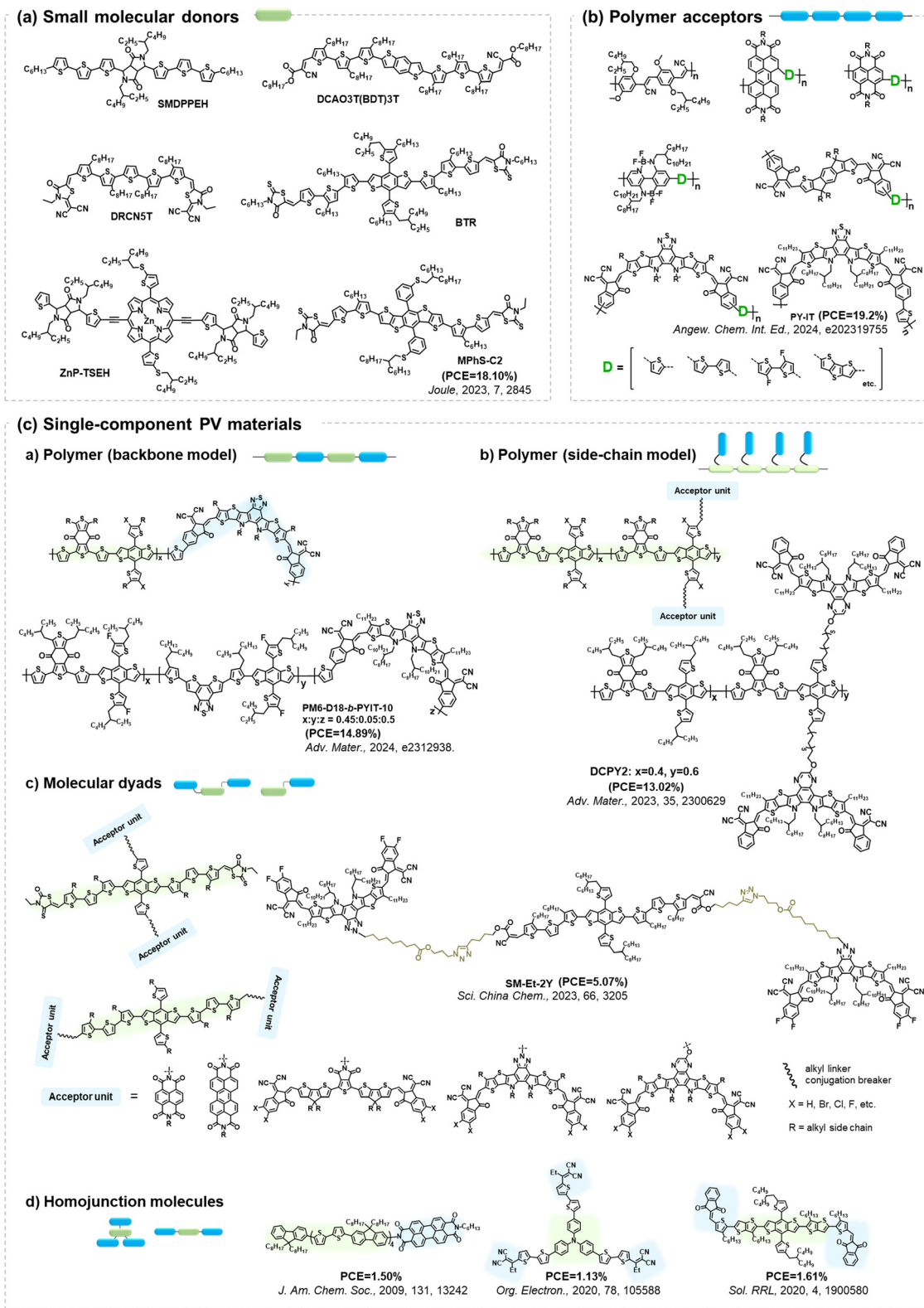
Fig. 24 Molecular architectures of representative PV materials in Fig. 23 (Section 4). Despite advancements in PCEs and reporting device stability/lifetime, studies on the precise photochemical degradation pathways of these PV materials remain limited.

reactive compounds with NFAs. For fullerene-based OSCs, PEI/PEIE is a widely used material for doping or interface treatment to improve device performance.[201–203] However, when PEI/PEIE meets NFAs, a voltage drop occurs, leading to a typical "S"

7444 | *Chem. Soc. Rev.*, 2024, **53**, 7426–7454

This journal is © The Royal Society of Chemistry 2024

shape current–voltage (*J–V*) curves.[23,200,204] It was found that there are "toxic" chemical reactions between PEI/PEIE and NFAs.[200] As shown in Fig. 25(c), generally, the amine group acts as a nucleophile, engaging in an addition reaction with the vinyl group in NFAs. This reaction ultimately disrupts the double bond (vinyl linker) and the extensive conjugated structure of the molecule, leading to the loss of device performance.[23] Such "toxic" chemical reactions between amine-containing materials and NFAs can be efficiently suppressed by reducing the chemical reactivity of –NH groups, achieved through methods like metal ion-chelated PEI,[200,205] chelation with small molecules,[206,207] modification of the amine groups,[208,209] and protonation of the amino groups.[210]

Zhou *et al.* observed that NFAs also react chemically with bases.[211] Through the introduction of sodium hydroxide into the ITIC solution, OH anions function as nucleophiles under basic conditions, targeting the vinyl group and producing ITIC-OH (ITIC after OH⁻ addition). The colour of the solution transitions from blue to orange upon mixing ITIC with PEIE. Upon adding acetic acid to the ITIC-OH solution, ITIC-OH reverts to ITIC. This interconversion between ITIC and ITIC-OH is reversible under both acidic and basic conditions.

These existing chemical reactions between PV materials and additives suggest that the chemical stability of OSCs not only depends on the intrinsic chemical stability of PV molecules but is also influenced by the reactive additives utilized during the device fabrication process.

5.2 Photochemical degradation mechanisms and the light-induced morphological changes in OSCs

Thermally induced morphological stability, driven by thermal diffusion and crystallization processes, is a phenomenon related to heat stress.[27,35,36,212,213] In contrast, photostability is linked to light stress. Generally, light can trigger photochemical reactions, yielding photodegraded products that result in device degradation.[24] This process involves a photochemical reaction inducing molecular structural changes at the sub-nm scale.[30,37,80,81,107,109,111,112,143,144,146,148,214,215] Under illumination, morphological changes at nm-scale also occur, either due to molecular alterations or light-induced molecular movements at the nm-scale.[29,216–220] As depicted in Fig. 26, conducting thermal stability measurements at temperatures close to those during photostability measurements can aid in understanding thermally induced morphological effects. However, comprehending the light-induced changes at the sub-nm and nm scales requires further analysis to elucidate the photostability of OSCs.

In the era dominated by fullerene-based materials, the study of photostability is linked to the photochemical reactions and the related light-induced morphological changes. This connection arises from the reversible light-induced dimerization process experienced by fullerenes, which can be correlated with their morphological characteristics.[89,90] However, in the era of NFAs, the complexity of chemical reactions would complicate the light-induced morphological changes.[80] It is also reasonable that light-induced molecular changes
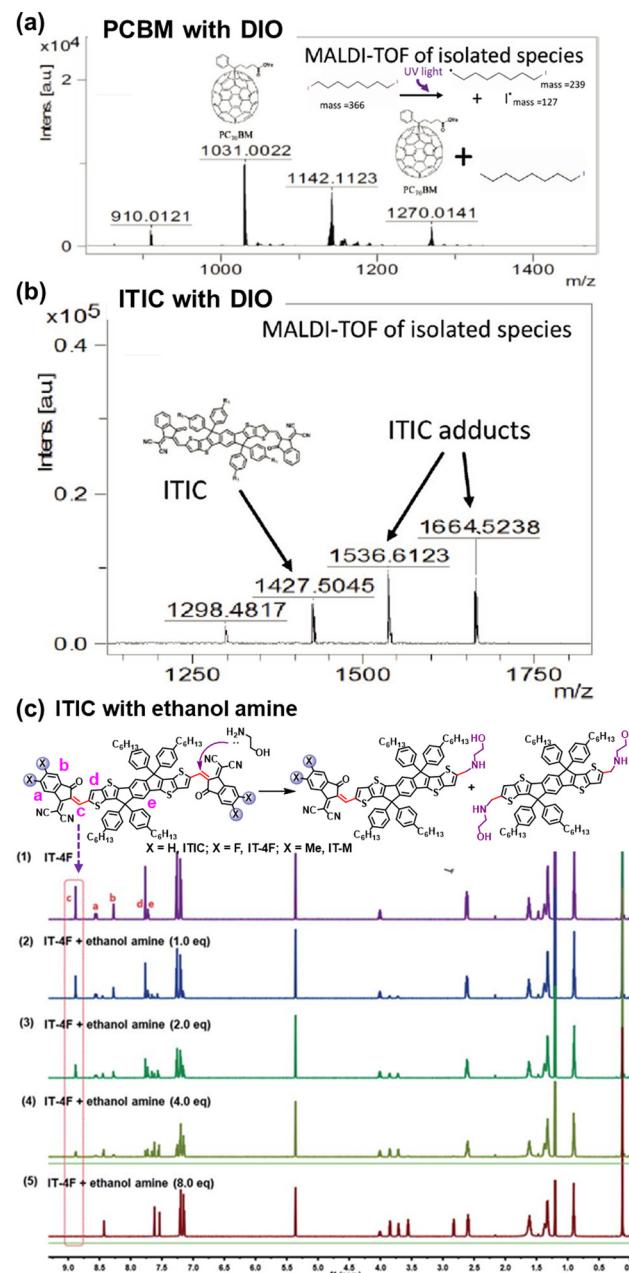
Fig. 25 Chemical reactions between photovoltaic materials and additives: (a) and (b) DIO and (c) PEI.[196,200] Reproduced from ref. 196 with permission from Wiley-VCH, Copyright 2019. Reproduced from ref. 200, CC BY.

(chemical degradation) at the sub-nm scale could trigger the morphological changes at the nm-scale.[29,216,220,221]

It is noteworthy that several research groups observed no clear or minor morphological changes in NFA-based OSCs during photostability measurements through techniques such as atomic force microscopy (AFM), grazing-incidence wide-angle X-ray scattering (GIWAXS), and grazing-incidence small-angle X-ray scattering (GISAXS).[39,114,149,217] Detecting mixed D : A domains in BHJ layers also remains a persistent challenge within the research community. These findings underscore the

This journal is © The Royal Society of Chemistry 2024

Chem. Soc. Rev., 2024, **53**, 7426–7454 | 7445
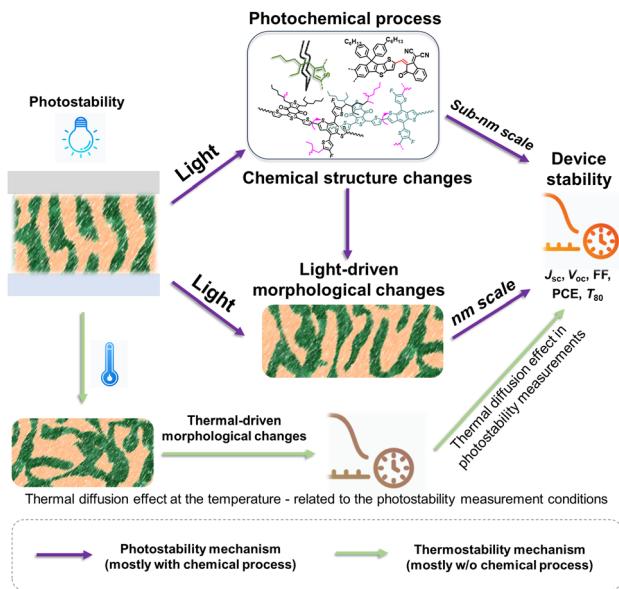
Fig. 26 The distinction and connection between the light-induced molecular structural changes (sub-nm scale) and light-driven morphological changes (nm scale), and the mechanism differences between photostability and thermal stability.

limitations of conventional morphological techniques in tracking the photodegradation behaviors in NFA-based devices. In a recent study, Müller-Buschbaum *et al.* employed AFM, GIWAXS, and GISAXS to investigate four distinct PM6-based devices incorporating Y6, ITIC-4F, ITIC-4Cl, and $PC_{71}BM$. While AFM and GIWAXS exhibited only minor changes during photoaging, notably, a clear trend of light-induced nm scale morphological changes emerged from operando-GISAXS measurements.[216]

This highlights the necessity of addressing the photochemically induced molecular changes at the sub-nanometer scale in conjunction with the light-induced nano-scale morphological changes.

6. Conclusions and outlooks

This review delves into the photodegradation mechanisms of electron acceptors and donors as photo-active layers in OSCs. As illustrated in Fig. 27, unlike thermal-induced morphological changes (mostly w/o a chemical process), the photostability of PV materials primarily encompasses photochemically induced molecular alterations at the sub-nanometer scale and the light-induced nano-scale morphological changes. Over the past decades, investigations into photochemical degradation pathways have predominantly employed polymer donors and NFAs as the model systems. Herein, we highlight the advancements in strategies aimed at enhancing the photochemical stability of OSCs from a chemical perspective, as depicted in Fig. 27.

(1) Enhancing the intrinsic photochemical stability of PV materials: (i) NFAs: Since the discoveries in organic semiconductors (Nobel lecture),[128] it has been well-established that vinyl groups (C=C bonds) exhibit considerable flexibility and susceptibility to isomerization reactions. Numerous studies have confirmed the vulnerability of the vinyl group as the weak link in NFAs as summarized in Section 2. Therefore, one effective strategy to enhance photostability involves circumventing the use of vinyl groups and employing approaches like the ring-lock strategy.[108,129,130] However, this necessitates a different molecular design concept for NFAs, particularly in the linking unit between core and end-group moieties. Another approach involves reinforcing resistance to isomerization
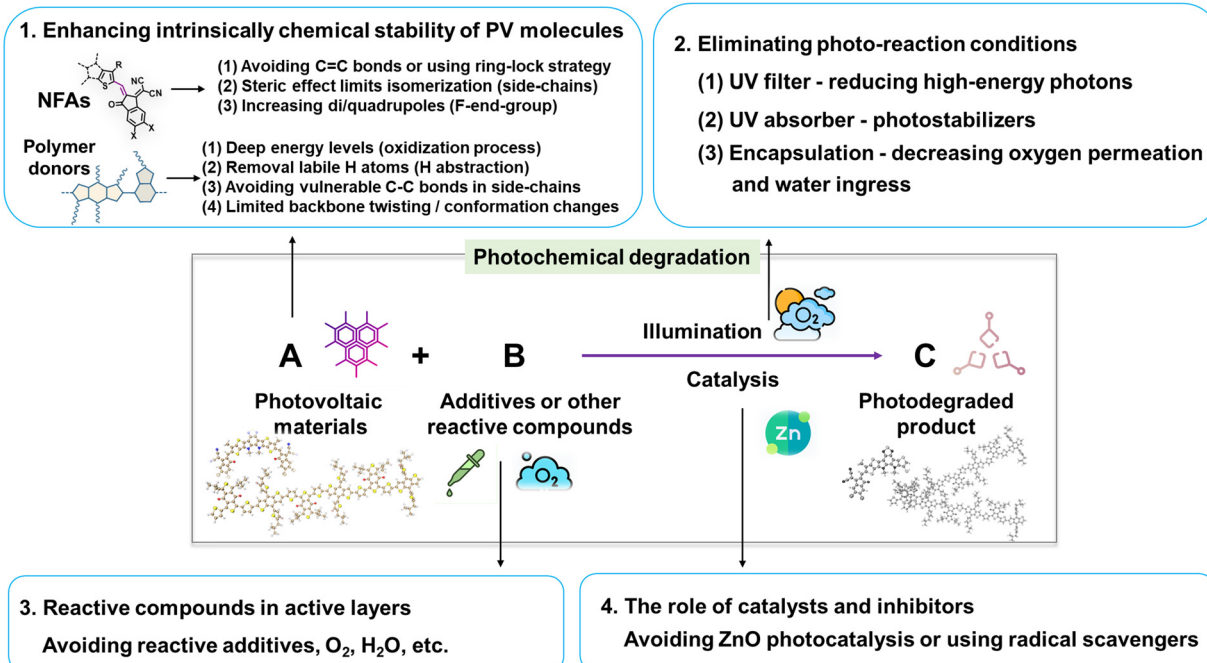
Fig. 27 Strategies for enhancing photostability of PV materials and the OSC devices.

7446 | *Chem. Soc. Rev.*, 2024, **53**, 7426–7454

This journal is © The Royal Society of Chemistry 2024

reactions, achieved through the use of steric side-chains (demonstrating improved photostability from ITIC to Y-NFAs *via* outer side-chains) and high di/quadrupoles in NFAs (enhancing stability through fluorinated end-groups).[25,106,122]

(ii) Polymer donors: under O_2 conditions, the deep energy levels of donors benefit in suppressing the oxidation process.[143] Notably, avoiding the use of BDT-thiophene units is also an effective strategy for limiting the backbone twisting effect in polymer donors (associated with device degradation).[29] Even in the absence of O_2 and H_2O, polymer donors are still susceptible to photodegradation through H-abstraction and homolytic scissions in side-chains, along with backbone twisting as summarized in Section 3. Hence, the necessity to avoid using labile H and vulnerable single chemical bonds (C–C/X, X as Cl, Br, *etc*) in side-chains persists in ensuring a restrained backbone conformation.

Other strategies are (2) Elimination of photoaging conditions: this involves the use of UV filters and UV absorber/stabilizers,[196,222] and coupled with high-quality encapsulation to prevent the ingress of O_2 and H_2O.[24,82] (3) Avoidance of reactive compounds: this includes refraining from using reactive components like DIO and reactive amines. (4) Catalysis and inhibitors: this entails refraining from the use of photocatalytic ZnO with UV light.[112] Additionally, incorporating radical scavengers is also an effective strategy in suppressing the photodegradation pathways in NFAs and polymer donors.[81,223]

In summary, while significant progress has been made in developing high-performance OSCs, achieving stable OSCs with high PCEs remains challenging.[224,225] Addressing these challenges requires enhancing device photostability while concurrently reducing the cost of PV materials. Future research endeavors should prioritize a deeper exploration of photochemical degradation pathways and the development of photostable and high-performance PV materials that are cost-effective and conducive to large-scale synthesis and green-solvent processability, thereby facilitating industrial-level scale-up and commercialization of OSCs.

Abbreviations

OSCs	Organic solar cells
D/A	Donor/acceptor
BHJ	Bulk heterojunction
PV	Photovoltaics
PCEs	Power conversion efficiencies
ISOS	International summit on organic photovoltaics
PCBM	Phenyl-C61-butyric acid methyl ester or phenyl-C71-butyric acid methyl ester, also known as $PC_{61}BM$ or $PC_{71}BM$
PDI	Perylenediimide
IDTBR	(5Z)-3-Ethyl-2-sulfanylidene-5-[[4-[9,9,18,18-tetrakis(R)-15-[7-[(Z)-(3-ethyl-4-oxo-2-sulfanylidene-1,3-thiazolidin-5-ylidene)methyl]-2,1,3-benzothiadiazol-4-yl]-5,14-dithiapentacyclo[10.6.0.0.3,100^{4,8}.0^{13,17}] octadeca-1(12),2,4(8),6,10,13(17),15-heptaen-6-
ITIC	yl]-2,1,3-benzothiadiazol-7-yl]methylidene]-1,3-thiazolidin-4-one; herein, R = *n*-octyl for O-IDTBR and R = 2-ethylhexyl for EH-IDTBR
ITIC	3,9-bis(2-Methylene-(3-(1,1-dicyanomethylene)-indanone)-5,5,11,11-tetrakis(4-hexylphenyl)-dithieno[2,3-*d*:2′,3′-*d*″]-*s*-indaceno[1,2-*b*:5,6-*b*]-dithiophene), also known as ITIC-H
BTP	Dithienothiophen[3.2-*b*]pyrrolobenzothiadiazole
BTP-4F	(2,20-((2Z,20Z)-((12,13-bis(2-Ethylhexyl)-3,9-diundecyl-12,13-dihydro-[1,2,5]thiadiazolo[3,4-*e*] thieno[2′″,30″:4′,50] thieno[20,30:4,5]pyrrolo [3,2-*g*]thieno[20,30:4,5] thieno[3,2-*b*]indole-2,10-diyl) bis(methanylylidene))bis(5,6-difluoro-3-oxo-2,3-dihydro-1*H*-indene-2,1-diylidene)) dimalononitrile), also known as Y6
MDMO-PPV	Poly[2-methoxy-5-(3′,7′-dimethyloctyloxy)-*p*-phenylene vinylene]
P3HT	Poly(3-hexylthiophene)
PM6	Poly[[2,6-(4,8-bis(5-(2-ethylhexyl-3-fluoro) thiophen-2-yl)-benzo[1,2-*b*:4,5-*b*′]dithiophene))-*alt*-(5,5-(1′,3′-di-2-thienyl-5′,7′-bis(2-ethylhexyl) benzo[1′,2′-*c*:4′,5′-*c*′]dithiophene-4,8-dione)]]
D18	Poly[[2,6-(4,8-bis(5-(2-ethylhexyl-3-fluoro)thiophen-2-yl)-benzo[1,2-*b*:4,5-*b*′]dithiophene))-*alt*-5,5′-(5,8-bis(4-(2-butyloctyl)thiophen-2-yl)dithieno [3′,2′:3,4;2″,3″:5,6]benzo[1,2-*c*][1,2,5] thiadiazole)]
MALDI-TOF	Matrix-assisted laser desorption/ionization – time of flight
UPS	Ultraviolet photoelectron spectroscopy
NEXAFS	Near-edge X-ray absorption fine structure
V_{OC}	Open-circuit voltage
J_{SC}	Short-circuit current density
FF	Fill factor
LUMO	Lowest unoccupied molecular orbital
HOMO	Highest occupied molecular orbital
Vis-NIR	Visible-near-infrared
NDI	Naphthalene diimide
IDT	Indacenodithiophene
FBR	5,5′-[(9,9-Dioctyl-9*H*-fluorene-2,7-diyl)bis(2,1,3-benzothiadiazole-7,4-diylmethylidyne)]bis[3-ethyl-2-thioxo-4-thiazolidinone]
IDFBR	(5Z)-3-Ethyl-5-[[4-[2-[7-[(Z)-(3-ethyl-4-oxo-2-sulfanylidene-1,3-thiazolidin-5-ylidene)methyl]-2,1,3-benzothiadiazol-4-yl]-6,6,12,12-tetraoctylindeno[1,2-*b*]fluoren-8-yl]-2,1,3-benzothiadiazol-7-yl]methylidene]-2-sulfanylidene-1,3-thiazolidin-4-one
NFAs	Non-fullerene acceptors
FT-IR	Fourier transform infrared absorption spectra
XPS	X-ray photoelectron spectroscopy
NMR	Nuclear magnetic resonance
ITIC-4F	3,9-bis(2-Methylene-((3-(1,1-dicyanomethylene)-6,7-difluoro-indanone))-5,5,11,11-tetrakis

This journal is © The Royal Society of Chemistry 2024

Chem. Soc. Rev., 2024, **53**, 7426–7454 | 7447

	(4-hexylphenyl)-dithieno[2,3-*d*:2′,3′-*d′*]-*s*-indaceno[1,2-*b*:5,6-*b′*]dithiophene, also known as IT-4F
ITIC-M	2-[(2*Z*)-2-[[20-[(*E*)-[1-(Dicyanomethylidene)-5,6-dimethyl-3-oxoinden-2-ylidene]methyl]-12,12,24,24-tetrakis(4-hexylphenyl)-5,9,17,21-tetrathiaheptacyclo[13.9.0.0.^{3,13}0.^{4,11}0^{6,10}.0.^{16,23}0^{18,22}]tetracosa-1(15),2,4(11),6(10),7,13,16(23),18(22),19-nonaen-8-yl]methylidene]-5,6-dimethyl-3-oxoinden-1-ylidene]propanedinitrile
ITIC-4Cl	3,9-bis(2-Methylene-((3-(1,1-dicyanomethylene)-chloro)-indanone))-5,5,11,11-tetrakis(4-hexylphenyl)-dithieno[2,3-*d*:2′,3′-*d′*]-*s*-indaceno [1,2-*b*:5,6-*b′*]dithiophene
DFT	Density functional theory
MS	Mass spectrometry
INCN	1,1-Dicyanomethylene-3-indanon
ETL	Electron transport layer
IEICO-4F	2,2′-[[4,4,9,9-tetrakis(4-hexylphenyl)-4,9-dihydro-*s*-indaceno[1,2-*b*:5,6-*b′*]dithiophene-2,7-diyl]bis[[4-[(2-ethylhexyl)oxy]-5,2-thiophenediyl]methylidyne(5,6-difluoro-3-oxo-1*H*-indene-2,1(3*H*)-diylidene)]]bis [propanedinitrile]
SAM	Self-assembled monolayer
PEDOT:PSS	Poly(3,4-ethylenedioxy-thiophene):poly(styrenesulfonate).
PTB7-Th	Poly([2,6′-4,8-di(5-ethylhexylthienyl)benzo[1,2-*b*;3,3-*b*]dithiophene])
PTQ10	Poly[(thiophene)-*alt*-(6,7-difluoro-2-(2-hexyldecyloxy)quinoxaline)]
ESR	Electron spin resonance
BDT	Thienyl-substituted-benzodithiophene
GPC	Gel permeation chromatography
CV	Cyclic voltammetry
DIO	1,8-Di-iodooctane
HPLC–MS	High performance liquid chromatography–mass spectrometry
PEI	Polyethylenimine
PEIE	Ethoxylated polyethylenimine
J–V	Current–voltage
AFM	Atomic force microscopy
GIWAXS	Grazing-incidence wide-angle X-ray scattering
GISAXS	Grazing-incidence small-angle X-ray scattering

Author contributions

J. H. prepared the first draft of the manuscript. S. K. P., H. X., A. S., and D. B. reviewed and revised the manuscript. D. B. supervised the project.

Conflicts of interest

There are no conflicts to declare.

Acknowledgements

Notes and references

1 H. Yu, J. Wang, Q. Zhou, J. Qin, Y. Wang, X. Lu and P. Cheng, *Chem. Soc. Rev.*, 2023, **52**, 4132–4148.

2 Y. Li, X. Huang, H. K. M. Sheriff and S. R. Forrest, *Nat. Rev. Mater.*, 2022, **8**, 186–201.

3 G. Zhang, F. R. Lin, F. Qi, T. Heumuller, A. Distler, H. J. Egelhaaf, N. Li, P. C. Y. Chow, C. J. Brabec, A. K. Jen and H. L. Yip, *Chem. Rev.*, 2022, **122**, 14180–14274.

4 D. Corzo, D. Rosas-Villalva, A. C, G. Tostado-Blázquez, E. B. Alexandre, L. H. Hernandez, J. Han, H. Xu, M. Babics, S. De Wolf and D. Baran, *Nat. Energy*, 2022, **8**, 62–73.

5 I. McCulloch, M. Chabinyc, C. Brabec, C. B. Nielsen and S. E. Watkins, *Nat. Mater.*, 2023, **22**, 1304–1310.

6 J. W. Lee, C. Sun, S. W. Lee, G. U. Kim, S. Li, C. Wang, T. S. Kim, Y. H. Kim and B. J. Kim, *Energy Environ. Sci.*, 2022, **15**, 4672–4685.

7 J.-W. Lee, H.-G. Lee, E. S. Oh, S.-W. Lee, T. N.-L. Phan, S. Li, T.-S. Kim and B. J. Kim, *Joule*, 2024, **8**, 204–223.

8 L. Zhu, M. Zhang, J. Xu, C. Li, J. Yan, G. Zhou, W. Zhong, T. Hao, J. Song, X. Xue, Z. Zhou, R. Zeng, H. Zhu, C. C. Chen, R. C. I. MacKenzie, Y. Zou, J. Nelson, Y. Zhang, Y. Sun and F. Liu, *Nat. Mater.*, 2022, **21**, 656–663.

9 Z. Zheng, J. Wang, P. Bi, J. Ren, Y. Wang, Y. Yang, X. Liu, S. Zhang and J. Hou, *Joule*, 2022, **6**, 171–184.

10 A. Wadsworth, M. Moser, A. Marks, M. S. Little, N. Gasparini, C. J. Brabec, D. Baran and I. McCulloch, *Chem. Soc. Rev.*, 2019, **48**, 1596–1625.

11 D. Meng, R. Zheng, Y. Zhao, E. Zhang, L. Dou and Y. Yang, *Adv. Mater.*, 2022, **34**, e2107330.

12 J. W. Lee, C. Sun, T. N. L. Phan, D. C. Lee, Z. Tan, H. Jeon, S. Cho, S. K. Kwon, Y. H. Kim and B. Kim, *Energy Environ. Sci.*, 2023, **16**, 3339–3349.

13 Y. Zhang, W. Deng, C. E. Petoukhoff, X. Xia, Y. Lang, H. Xia, H. Tang, H. T. Chandran, S. Mahadevan, K. Liu, P. W. K. Fong, Y. Luo, J. Wu, S.-W. Tsang, F. Laquai, H. Wu, X. Lu, Y. Yang and G. Li, *Joule*, 2024, **8**, 509–526.

14 J. W. Lee, J. S. Park, H. Jeon, S. Lee, D. Jeong, C. Lee, Y. H. Kim and B. J. Kim, *Chem. Soc. Rev.*, 2024, **53**, 4674–4706.

15 S. Karuthedath, J. Gorenflot, Y. Firdaus, N. Chaturvedi, C. S. P. De Castro, G. T. Harrison, J. I. Khan, A. Markina, A. H. Balawi, T. A. D. Pena, W. Liu, R. Z. Liang, A. Sharma, S. H. K. Paleti, W. Zhang, Y. Lin, E. Alarousu, S. Lopatin,

7448 | *Chem. Soc. Rev.*, 2024, **53**, 7426–7454

This journal is © The Royal Society of Chemistry 2024

D. H. Anjum, P. M. Beaujuge, S. De Wolf, I. McCulloch, T. D. Anthopoulos, D. Baran, D. Andrienko and F. Laquai, *Nat. Mater.*, 2022, **21**, 378.

16 J. Yi, G. Zhang, H. Yu and H. Yan, *Nat. Rev. Mater.*, 2023, **9**, 46–62.

17 N. Gasparini, A. Salleo, I. McCulloch and D. Baran, *Nat. Rev. Mater.*, 2019, **4**, 229–242.

18 D. Baran, R. S. Ashraf, D. A. Hanifi, M. Abdelsamie, N. Gasparini, J. A. Rohr, S. Holliday, A. Wadsworth, S. Lockett, M. Neophytou, C. J. Emmott, J. Nelson, C. J. Brabec, A. Amassian, A. Salleo, T. Kirchartz, J. R. Durrant and I. McCulloch, *Nat. Mater.*, 2017, **16**, 363–369.

19 L. Wang, C. Chen, Y. W. Fu, C. H. Guo, D. H. Li, J. C. Cheng, W. Sun, Z. R. Gan, Y. D. Sun, B. J. Zhou, C. H. Liu, D. Liu, W. Li and T. Wang, *Nat. Energy*, 2024, **9**, 208–218.

20 J. Hou, O. Inganas, R. H. Friend and F. Gao, *Nat. Mater.*, 2018, **17**, 119–128.

21 M. Riede, D. Spoltore and K. Leo, *Adv. Energy Mater.*, 2020, **11**, 2002653.

22 B. Azzopardi, C. J. M. Emmott, A. Urbina, F. C. Krebs, J. Mutale and J. Nelson, *Energy Environ. Sci.*, 2011, **4**, 3741–3753.

23 P. Jiang, L. Hu, L. Sun, Z. Li, H. Han and Y. Zhou, *Chem. Sci.*, 2022, **13**, 4714–4739.

24 P. Cheng and X. Zhan, *Chem. Soc. Rev.*, 2016, **45**, 2544–2582.

25 J. Luke, E. J. Yang, C. Labanti, S. Y. Park and J. S. Kim, *Nat. Rev. Mater.*, 2023, **8**, 839–852.

26 P. Ding, D. Yang, S. Yang and Z. Ge, *Chem. Soc. Rev.*, 2024, **53**, 2350–2387.

27 Z. X. Peng, N. Stingelin, H. Ade and J. J. Michels, *Nat. Rev. Mater.*, 2023, **8**, 439–455.

28 L. Lüer, I. M. Peters, A. S. Smith, E. Dorschky, B. M. Eskofier, F. Liers, J. Franke, M. Sjarov, M. Brossog, D. M. Guldi, A. Maier and C. J. Brabec, *Joule*, 2024, **8**, 295–311.

29 Y. W. Wang, J. Luke, A. Privitera, N. Rolland, C. Labanti, G. Londi, V. Lemaur, D. T. W. Toolan, A. J. Sneyd, S. Jeong, D. P. Qian, Y. Olivier, L. Sorace, J. S. Kim, D. Beljonne, Z. Li and A. J. Gillett, *Joule*, 2023, **7**, 810–829.

30 Y. W. Li, T. F. Li and Y. Z. Lin, *Mater. Chem. Front.*, 2021, **5**, 2907–2930.

31 M. O. Reese, S. A. Gevorgyan, M. Jorgensen, E. Bundgaard, S. R. Kurtz, D. S. Ginley, D. C. Olson, M. T. Lloyd, P. Moryillo, E. A. Katz, A. Elschner, O. Haillant, T. R. Currier, V. Shrotriya, M. Hermenau, M. Riede, K. R. Kirov, G. Trimmel, T. Rath, O. Inganäs, F. L. Zhang, M. Andersson, K. Tvingstedt, M. Lira-Cantu, D. Laird, C. McGuiness, S. Gowrisanker, M. Pannone, M. Xiao, J. Hauch, R. Steim, D. M. DeLongchamp, R. Rösch, H. Hoppe, N. Espinosa, A. Urbina, G. Yaman-Uzunoglu, J. B. Bonekamp, A. J. J. M. van Breemen, C. Girotto, E. Voroshazi and F. C. Krebs, *Sol. Energy Mater. Sol. Cells*, 2011, **95**, 1253–1267.

32 Y. Zhang, I. D. W. Samuel, T. Wang and D. G. Lidzey, *Adv. Sci.*, 2018, **5**, 1800434.

33 L. Duan and A. Uddin, *Adv. Sci.*, 2020, **7**, 1903259.

34 G. Tregnago, *Nat. Energy*, 2022, **7**, 567.

35 M. Ghasemi, N. Balar, Z. Peng, H. Hu, Y. Qin, T. Kim, J. J. Rech, M. Bidwell, W. Mask, I. McCulloch, W. You, A. Amassian, C. Risko, B. T. O'Connor and H. Ade, *Nat. Mater.*, 2021, **20**, 525–532.

36 S. Siddika, Z. X. Peng, N. Balar, X. Y. Dong, X. W. Zhong, W. You, H. Ade and B. T. O'Connor, *Joule*, 2023, **7**, 1593–1608.

37 Y. Che, M. R. Niazi, R. Izquierdo and D. F. Perepichka, *Angew. Chem., Int. Ed.*, 2021, **60**, 24833–24837.

38 H. K. H. Lee, A. M. Telford, J. A. Röhr, M. F. Wyatt, B. Rice, J. Y. Wu, A. D. Maciel, S. M. Tuladhar, E. Speller, J. McGettrick, J. R. Searle, S. Pont, T. Watson, T. Kirchartz, J. R. Durrant, W. C. Tsoi, J. Nelson and Z. Li, *Energy Environ. Sci.*, 2018, **11**, 417–428.

39 T. R. Liu, Q. C. Burlingame, M. R. Ivancevic, X. Liu, J. N. Hu, B. P. Rand and Y. L. Loo, *Adv. Energy Mater.*, 2023, **13**, 2300046.

40 O. R. Yamilova, I. V. Martynov, A. S. Brandvold, I. V. Klimovich, A. H. Balzer, A. V. Akkuratov, I. E. Kusnetsov, N. Stingelin and P. A. Troshin, *Adv. Energy Mater.*, 2020, **10**, 1903163.

41 N. Yang, Y. Cui, T. Zhang, C. An, Z. Chen, Y. Xiao, Y. Yu, Y. Wang, X.-T. Hao and J. Hou, *J. Am. Chem. Soc.*, 2024, **146**, 9205–9215.

42 Y. Liang, D. Zhang, Z. Wu, T. Jia, L. Lüer, H. Tang, L. Hong, J. Zhang, K. Zhang, C. J. Brabec, N. Li and F. Huang, *Nat. Energy*, 2022, **7**, 1180–1190.

43 X. Gu, R. Zeng, T. He, G. Zhou, C. Li, N. Yu, F. Han, Y. Hou, J. Lv, M. Zhang, J. Zhang, Z. Wei, Z. Tang, H. Zhu, Y. Cai, G. Long, F. Liu, X. Zhang and H. Huang, *Adv. Mater.*, 2024, e2401370.

44 J. J. M. Halls, C. A. Walsh, N. C. Greenham, E. A. Marseglia, R. H. Friend, S. C. Moratti and A. B. Holmes, *Nature*, 1995, **376**, 498–500.

45 G. Yu, J. Gao, J. C. Hummelen, F. Wudl and A. J. Heeger, *Science*, 1995, **270**, 1789–1791.

46 G. Li, V. Shrotriya, J. S. Huang, Y. Yao, T. Moriarty, K. Emery and Y. Yang, *Nat. Mater.*, 2005, **4**, 864–868.

47 D. Mühlbacher, M. Scharber, M. Morana, C. Brabec, Z. Zhu, D. Waller and R. Gaudiana, *Adv. Mater.*, 2006, **18**, 2884–2889.

48 Y. Sun, C. Cui, H. Wang and Y. Li, *Adv. Energy Mater.*, 2011, **1**, 1058–1061.

49 Q. F. Yan, Y. Zhou, Y. Q. Zheng, J. Pei and D. H. Zhao, *Chem. Sci.*, 2013, **4**, 4389–4394.

50 J. D. Chen, C. Cui, Y. Q. Li, L. Zhou, Q. D. Ou, C. Li, Y. Li and J. X. Tang, *Adv. Mater.*, 2015, **27**, 1035–1041.

51 S. Holliday, R. S. Ashraf, C. B. Nielsen, M. Kirkus, J. A. Rohr, C. H. Tan, E. Collado-Fregoso, A. C. Knall, J. R. Durrant, J. Nelson and I. McCulloch, *J. Am. Chem. Soc.*, 2015, **137**, 898–904.

52 Y. Lin, J. Wang, Z. G. Zhang, H. Bai, Y. Li, D. Zhu and X. Zhan, *Adv. Mater.*, 2015, **27**, 1170–1174.

This journal is © The Royal Society of Chemistry 2024

Chem. Soc. Rev., 2024, **53**, 7426–7454 | 7449

53 D. Baran, T. Kirchartz, S. Wheeler, S. Dimitrov, M. Abdelsamie, J. Gorman, R. S. Ashraf, S. Holliday, A. Wadsworth and N. Gasparini, *Energy Environ. Sci.*, 2016, **9**, 3783–3793.

54 S. Holliday, R. S. Ashraf, A. Wadsworth, D. Baran, S. A. Yousaf, C. B. Nielsen, C. H. Tan, S. D. Dimitrov, Z. Shang, N. Gasparini, M. Alamoudi, F. Laquai, C. J. Brabec, A. Salleo, J. R. Durrant and I. McCulloch, *Nat. Commun.*, 2016, **7**, 11585.

55 W. Zhao, D. Qian, S. Zhang, S. Li, O. Inganas, F. Gao and J. Hou, *Adv. Mater.*, 2016, **28**, 4734–4739.

56 S. Li, L. Zhan, F. Liu, J. Ren, M. Shi, C. Z. Li, T. P. Russell and H. Chen, *Adv. Mater.*, 2018, **30**, 1705208.

57 W. Li, L. Ye, S. Li, H. Yao, H. Ade and J. Hou, *Adv. Mater.*, 2018, **30**, 1707170.

58 L. Meng, Y. Zhang, X. Wan, C. Li, X. Zhang, Y. Wang, X. Ke, Z. Xiao, L. Ding, R. Xia, H. L. Yip, Y. Cao and Y. Chen, *Science*, 2018, **361**, 1094–1098.

59 Q. Liu, Y. Jiang, K. Jin, J. Qin, J. Xu, W. Li, J. Xiong, J. Liu, Z. Xiao, K. Sun, S. Yang, X. Zhang and L. Ding, *Sci. Bull.*, 2020, **65**, 272–275.

60 C. Li, J. Zhou, J. Song, J. Xu, H. Zhang, X. Zhang, J. Guo, L. Zhu, D. Wei, G. Han, J. Min, Y. Zhang, Z. Xie, Y. Yi, H. Yan, F. Gao, F. Liu and Y. Sun, *Nat. Energy*, 2021, **6**, 605–613.

61 T. Lin, Y. Hai, Y. Luo, L. Feng, T. Jia, J. Wu, R. Ma, T. A. Dela Pena, Y. Li, Z. Xing, M. Li, M. Wang, B. Xiao, K. S. Wong, S. Liu and G. Li, *Adv. Mater.*, 2024, e2312311.

62 M. Lv, Q. Wang, J. Zhang, Y. Wang, Z. G. Zhang, T. Wang, H. Zhang, K. Lu, Z. Wei and D. Deng, *Adv. Mater.*, 2024, **36**, e2310046.

63 J. Yuan, Y. Zhang, L. Zhou, G. Zhang, H.-L. Yip, T.-K. Lau, X. Lu, C. Zhu, H. Peng, P. A. Johnson, M. Leclerc, Y. Cao, J. Ulanski, Y. Li and Y. Zou, *Joule*, 2019, **3**, 1140–1151.

64 D. Meng, H. T. Fu, C. Y. Xiao, X. Y. Meng, T. Winands, W. Ma, W. Wei, B. B. Fan, L. J. Huo, N. L. Doltsinis, Y. Li, Y. M. Sun and Z. H. Wang, *J. Am. Chem. Soc.*, 2016, **138**, 10184–10190.

65 L. Ma, S. Zhang, J. Zhu, J. Wang, J. Ren, J. Zhang and J. Hou, *Nat. Commun.*, 2021, **12**, 5093.

66 A. Mishra and G. D. Sharma, *Angew. Chem., Int. Ed.*, 2023, **62**, e202219245.

67 X. Zhang, X. Gu and H. Huang, *Acc. Chem. Res.*, 2024, **57**, 981–991.

68 D. Luo, C. J. Brabec and A. K. K. Kyaw, *Nano Energy*, 2023, **114**, 108661.

69 Z. P. Yu, Z. X. Liu, F. X. Chen, R. Qin, T. K. Lau, J. L. Yin, X. Kong, X. Lu, M. Shi, C. Z. Li and H. Chen, *Nat. Commun.*, 2019, **10**, 2152.

70 D. L. Ma, Q. Q. Zhang and C. Z. Li, *Angew. Chem., Int. Ed.*, 2023, **62**, e202214931.

71 J. Wang, Q. Luan, P. Wang, C. Han, F. Bi, C. Yang, Y. Li and X. Bao, *Adv. Funct. Mater.*, 2023, **33**, 2301575.

72 L. J. Bu, X. Y. Guo, B. Yu, Y. Qu, Z. Y. Xie, D. H. Yan, Y. H. Geng and F. S. Wang, *J. Am. Chem. Soc.*, 2009, **131**, 13242–13243.

73 H. Bai, Q. Fan, R. Ma, X. Guo, W. Ma and M. Zhang, *Chin. J. Chem.*, 2024, **42**, 1307–1318.

74 F. Qi, Y. Li, F. R. Lin and A. K. Jen, *ChemSusChem*, 2024, e202301559.

75 C. Sun, J.-W. Lee, C. Lee, D. Lee, S. Cho, S.-K. Kwon, B. J. Kim and Y.-H. Kim, *Joule*, 2023, **7**, 416–430.

76 C. Sun, J. W. Lee, Z. Tan, T. N. L. Phan, D. Han, H. G. Lee, S. Lee, S. K. Kwon, B. J. Kim and Y. H. Kim, *Adv. Energy Mater.*, 2023, **13**, 2301283.

77 J. W. Lee, C. Sun, J. Lee, D. J. Kim, W. J. Kang, S. Lee, D. Kim, J. Park, T. N. L. Phan, Z. Tan, F. S. Kim, J. Y. Lee, X. Bao, T. S. Kim, Y. H. Kim and B. J. Kim, *Adv. Energy Mater.*, 2024, **14**, 2303872.

78 D. W. Li, H. R. Zhang, X. Y. Cui, Y. N. Chen, N. Wei, G. L. Ran, H. Lu, S. H. Chen, W. K. Zhang, C. H. Li, Y. H. Liu, Y. Q. Liu and Z. S. Bo, *Adv. Mater.*, 2024, **36**, 2310362.

79 N. Yang, Y. Cui, Y. Xiao, Z. Chen, T. Zhang, Y. Yu, J. Ren, W. Wang, L. Ma and J. Hou, *Angew. Chem., Int. Ed.*, 2024, e202403753.

80 Y. Che, M. R. Niazi, Q. Chan, P. Ghamari, T. Yu, C. Ruchlin, H. Yu, H. Yan, D. Ma, S. S. Xiao, R. Izquierdo and D. F. Perepichka, *Angew. Chem., Int. Ed.*, 2023, **62**, e202309003.

81 J. Guo, Y. Wu, R. Sun, W. Wang, J. Guo, Q. Wu, X. F. Tang, C. K. Sun, Z. H. Luo, K. Chang, Z. H. Zhang, J. Yuan, T. F. Li, W. H. Tang, E. J. Zhou, Z. Xiao, L. M. Ding, Y. P. Zou, X. W. Zhan, C. L. Yang, Z. Li, C. J. Brabec, Y. F. Li and J. Min, *J. Mater. Chem. A*, 2019, **7**, 25088–25101.

82 R. Azmi, E. Ugur, A. Seitkhan, F. Aljamaan, A. S. Subbiah, J. Liu, G. T. Harrison, M. I. Nugraha, M. K. Eswaran, M. Babics, Y. Chen, F. Xu, T. G. Allen, A. U. Rehman, C. L. Wang, T. D. Anthopoulos, U. Schwingenschlogl, M. De Bastiani, E. Aydin and S. De Wolf, *Science*, 2022, **376**, 73–77.

83 H. Xu, J. H. Han, S. Chen, Y. Liu, L. H. Hernandez, J. Bertrandie, M. Babics, S. Alam, D. R. Villalva, S. H. K. Paleti, J. Gorenflot, C. Herok, N. Ramos, J. Troughton, A. Sharma, T. B. Marder, B. Engels, J. Martin, S. De Wolf, F. Laquai and D. Baran, *Joule*, 2023, **7**, 2135–2151.

84 F. L. Zhang, O. Inganäs, Y. H. Zhou and K. Vandewal, *Nat. Sci. Rev.*, 2016, **3**, 222–239.

85 J. B. Zhao, Y. K. Li, G. F. Yang, K. Jiang, H. R. Lin, H. Ade, W. Ma and H. Yan, *Nat. Energy*, 2016, **1**, 1–7.

86 A. S. Anselmo, A. Dzwilewski, K. Svensson and E. Moons, *Chem. Phys. Lett.*, 2016, **652**, 220–224.

87 S. Pont, S. Osella, A. Smith, A. V. Marsh, Z. Li, D. Beljonne, J. T. Cabral and J. R. Durrant, *Chem. Mater.*, 2019, **31**, 6076–6083.

88 E. M. Speller, A. J. Clarke, N. Aristidou, M. F. Wyatt, L. Francas, G. Fish, H. Cha, H. K. H. Lee, J. Luke, A. Wadsworth, A. D. Evans, I. McCulloch, J. S. Kim, S. A. Haque, J. R. Durrant, S. D. Dimitrov, W. C. Tsoi and Z. Li, *ACS Energy Lett.*, 2019, **4**, 846–852.

89 S. Pont, J. R. Durrant and J. T. Cabral, *Adv. Energy Mater.*, 2019, **9**, 1803948.

7450 | *Chem. Soc. Rev.*, 2024, **53**, 7426–7454

This journal is © The Royal Society of Chemistry 2024

90 H. C. Wong, Z. Li, C. H. Tan, H. Zhong, Z. Huang, H. Bronstein, I. McCulloch, J. T. Cabral and J. R. Durrant, *ACS Nano*, 2014, **8**, 1297–1308.

91 T. Heumueller, W. R. Mateker, A. Distler, U. F. Fritze, R. Cheacharoen, W. H. Nguyen, M. Biele, M. Salvador, M. von Delius, H. J. Egelhaaf, M. D. McGehee and C. J. Brabec, *Energy Environ. Sci.*, 2016, **9**, 247–256.

92 D. Lee, Y. Jang, J. Kim, S. Y. Jeong, H. Y. Woo, D. G. Lee, J. Kim, Y. Lee, C. Lee and W. Lee, *J. Mater. Chem. A*, 2023, **11**, 3008–3017.

93 L. Yu, D. Qian, S. Marina, F. A. A. Nugroho, A. Sharma, S. Hultmark, A. I. Hofmann, R. Kroon, J. Benduhn, D. M. Smilgies, K. Vandewal, M. R. Andersson, C. Langhammer, J. Martin, F. Gao and C. Muller, *ACS Appl. Mater. Interfaces*, 2019, **11**, 21766–21774.

94 O. Almora, D. Baran, G. C. Bazan, C. I. Cabrera, S. Erten-Ela, K. Forberich, F. Guo, J. Hauch, A. W. Y. Ho-Baillie, T. J. Jacobsson, R. A. J. Janssen, T. Kirchartz, N. Kopidakis, M. A. Loi, R. R. Lunt, X. Mathew, M. D. McGehee, J. Min, D. B. Mitzi, M. K. Nazeeruddin, J. Nelson, A. F. Nogueira, U. W. Paetzold, B. P. Rand, U. Rau, H. J. Snaith, E. Unger, L. Vaillant-Roca, C. Yang, H. L. Yip and C. J. Brabec, *Adv. Energy Mater.*, 2023, **13**, 2203313.

95 O. Almora, D. Baran, G. C. Bazan, C. Berger, C. Cabrera, K. R. Catchpole, S. Erten-Ela, F. Guo, J. Hauch, A. W. Y. Ho-Baillie, T. J. Jacobsson, R. A. J. Janssen, T. Kirchartz, N. Kopidakis, Y. F. Li, M. A. Loi, R. R. Lunt, X. Mathew, M. D. McGehee, J. Min, D. B. Mitzi, M. K. Nazeeruddin, J. Nelson, A. F. Nogueira, U. W. Paetzold, N. G. Park, B. P. Rand, U. Rau, H. J. Snaith, E. Unger, L. Vaillant-Roca, H. L. Yip and C. J. Brabec, *Adv. Energy Mater.*, 2021, **11**, 2102526.

96 O. Almora, D. Baran, G. C. Bazan, C. Berger, C. I. Cabrera, K. R. Catchpole, S. Erten-Ela, F. Guo, J. Hauch, A. W. Y. Ho-Baillie, T. J. Jacobsson, R. A. J. Janssen, T. Kirchartz, N. Kopidakis, Y. Li, M. A. Loi, R. R. Lunt, X. Mathew, M. D. McGehee, J. Min, D. B. Mitzi, M. K. Nazeeruddin, J. Nelson, A. F. Nogueira, U. W. Paetzold, N. G. Park, B. P. Rand, U. Rau, H. J. Snaith, E. Unger, L. Vaillant-Roca, H. L. Yip and C. J. Brabec, *Adv. Energy Mater.*, 2020, **11**, 2002774.

97 Y. Z. Lin and X. W. Zhan, *Mater. Horiz.*, 2014, **1**, 470–488.

98 J. Wang and X. Zhan, *Acc. Chem. Res.*, 2021, **54**, 132–143.

99 S. Chen, D. Meng, J. Huang, N. Liang, Y. Li, F. Liu, H. Yan and Z. Wang, *CCS Chem.*, 2021, **3**, 78–84.

100 C. Yan, S. Barlow, Z. Wang, H. Yan, A. K. Y. Jen, S. R. Marder and X. Zhan, *Nat. Rev. Mater.*, 2018, **3**, 18003.

101 S. Kumar, J. Shukla, Y. Kumar and P. Mukhopadhyay, *Org. Chem. Front.*, 2018, **5**, 2254–2276.

102 X. Guo, A. Facchetti and T. J. Marks, *Chem. Rev.*, 2014, **114**, 8943–9021.

103 J. Yao, Q. Chen, C. Zhang, Z. G. Zhang and Y. F. Li, *Susmat*, 2022, **2**, 243–263.

104 M. Sadeghianlemraski, C. R. Harding, G. C. Welch and H. Aziz, *ACS Appl. Energy Mater.*, 2020, **3**, 11655–11665.

105 A. Wadsworth, R. S. Ashraf, M. Abdelsamie, S. Pont, M. Little, M. Moser, Z. Hamid, M. Neophytou, W. M. Zhang, A. Amassian, J. R. Durrant, D. Baran and I. McCulloch, *ACS Energy Lett.*, 2017, **2**, 1494–1500.

106 J. Luke, E. M. Speller, A. Wadsworth, M. F. Wyatt, S. Dimitrov, H. K. H. Lee, Z. Li, W. C. Tsoi, I. McCulloch, D. Bagnis, J. R. Durrant and J. S. Kim, *Adv. Energy Mater.*, 2019, **9**, 1803755.

107 J. Guo, Y. Wu, R. Sun, W. Wang, J. F. Li, E. J. Zhou, J. Guo, T. Wang, Q. Wu, Z. H. Luo, W. Gao, Y. M. Pan, C. L. Yang and J. Min, *Sol. RRL*, 2021, **5**, 2000704.

108 H. T. Liu, W. Wang, Y. H. Zhou and Z. A. Li, *J. Mater. Chem. A*, 2021, **9**, 1080–1088.

109 Z. X. Liu, Z. P. Yu, Z. Shen, C. He, T. K. Lau, Z. Chen, H. Zhu, X. Lu, Z. Xie, H. Chen and C. Z. Li, *Nat. Commun.*, 2021, **12**, 3049.

110 A. J. Clarke, J. Luke, R. Meitzner, J. Y. Wu, Y. M. Wang, H. K. H. Lee, E. M. Speller, H. Bristow, Y. J. Cha, M. J. Newman, K. Hooper, A. Evans, F. Gao, H. Hoppe, I. McCulloch, U. S. Schubert, T. M. Watson, J. R. Durrant, W. C. Tsoi, J. S. Kim and Z. Li, *Cell Rep. Phys. Sci.*, 2021, **2**, 100498.

111 P. Das, C. T. Kornman, I. Ghiviriga, K. A. Abboud and R. K. Castellano, *Chem. Mater.*, 2023, **35**, 8122–8134.

112 Y. Y. Jiang, L. L. Sun, F. Y. Jiang, C. Xie, L. Hu, X. Y. Dong, F. Qin, T. F. Liu, L. Hu, X. S. Jiang and Y. H. Zhou, *Mater. Horiz.*, 2019, **6**, 1438–1443.

113 S. Park and H. J. Son, *J. Mater. Chem. A*, 2019, **7**, 25830–25837.

114 M. Gunther, D. Blatte, A. L. Oechsle, S. S. Rivas, A. A. Yousefi Amin, P. Muller-Buschbaum, T. Bein and T. Ameri, *ACS Appl. Mater. Interfaces*, 2021, **13**, 19072–19084.

115 L. Y. Su, H. H. Huang, C. E. Tsai, C. H. Hou, J. J. Shyue, C. H. Lu, C. W. Pao, M. H. Yu, L. Wang and C. C. Chueh, *Small*, 2022, **18**, e2107834.

116 S. Balasubramanian, M. A. Leon-Luna, B. Romero, M. Madsen and V. Turkovic, *ACS Appl. Mater. Interfaces*, 2023, **15**, 39647–39656.

117 S. Guan, Y. Li, C. Xu, N. Yin, C. Xu, C. Wang, M. Wang, Y. Xu, Q. Chen, D. Wang, L. Zuo and H. Chen, *Adv. Mater.*, 2024, e2400342.

118 S. Shoaee, H. M. Luong, J. Song, Y. Zou, T. Q. Nguyen and D. Neher, *Adv. Mater.*, 2023, e2302005.

119 S. X. Li, C. Z. Li, M. M. Shi and H. Z. Chen, *ACS Energy Lett.*, 2020, **5**, 1554–1567.

120 Q. Y. Wei, W. Liu, M. Leclerc, J. Yuan, H. G. Chen and Y. P. Zou, *Sci. China: Chem.*, 2020, **63**, 1352–1366.

121 J. Wang, Z. Zheng, Y. Zu, Y. Wang, X. Liu, S. Zhang, M. Zhang and J. Hou, *Adv. Mater.*, 2021, **33**, e2102787.

122 J. Luke, E. J. Yang, Y. C. Chin, Y. X. Che, L. Winkler, D. Whatling, C. Labanti, S. Y. Park and J. S. Kim, *Adv. Energy Mater.*, 2022, **12**, 2201267.

123 B. J. Zhou, L. Wang, Y. Liu, C. H. Guo, D. H. Li, J. L. Cai, Y. W. Fu, C. Chen, D. Liu, Y. H. Zhou, W. Li and T. Wang, *Adv. Funct. Mater.*, 2022, **32**, 2206042.

This journal is © The Royal Society of Chemistry 2024

Chem. Soc. Rev., 2024, **53**, 7426–7454 | 7451

124 B. Fan, W. Gao, R. Zhang, W. Kaminsky, F. R. Lin, X. Xia, Q. Fan, Y. Li, Y. An, Y. Wu, M. Liu, X. Lu, W. J. Li, H. L. Yip, F. Gao and A. K. Jen, *J. Am. Chem. Soc.*, 2023, **145**, 5909–5919.

125 B. Fan, W. Gao, X. Wu, X. Xia, Y. Wu, F. R. Lin, Q. Fan, X. Lu, W. J. Li, W. Ma and A. K. Jen, *Nat. Commun.*, 2022, **13**, 5946.

126 Y. S. Zhao, Z. N. Wu, X. Liu, Z. P. Zhong, R. H. Zhu and J. S. Yu, *J. Mater. Chem. C*, 2021, **9**, 13972–13980.

127 W. Q. Zhang, X. Y. Du, Y. L. Ma, J. W. Qiao, Q. D. Zheng and X. T. Hao, *Adv. Funct. Mater.*, 2024, **34**, 2308591.

128 H. Shirakawa, *Angew. Chem., Int. Ed.*, 2001, **40**, 2574–2580.

129 X. Zhu, S. Liu, Q. Yue, W. Liu, S. Sun and S. Xu, *CCS Chem.*, 2021, **3**, 1070–1080.

130 W. Liu, S. Xu, H. Lai, W. Liu, F. He and X. Zhu, *CCS Chem.*, 2023, **5**, 654–668.

131 S. Holliday, Y. L. Li and C. K. Luscombe, *Prog. Polym. Sci.*, 2017, **70**, 34–51.

132 N. S. Sariciftci, L. Smilowitz, A. J. Heeger and F. Wudl, *Science*, 1992, **258**, 1474–1476.

133 Z. Zheng, H. Yao, L. Ye, Y. Xu, S. Zhang and J. Hou, *Mater. Today*, 2020, **35**, 115–130.

134 C. An and J. Hou, *Acc. Mater. Res.*, 2022, **3**, 540–551.

135 Z. Wang, Z. Peng, Z. Xiao, D. Seyitliyev, K. Gundogdu, L. Ding and H. Ade, *Adv. Mater.*, 2020, **32**, e2005386.

136 M. Manceau, A. Rivaton, J. L. Gardette, S. Guillerez and N. Lemaître, *Polym. Degrad. Stab.*, 2009, **94**, 898–907.

137 H. Hintz, H. J. Egelhaaf, L. Lüer, J. Hauch, H. Peisert and T. Chassé, *Chem. Mater.*, 2010, **23**, 145–154.

138 M. Manceau, S. Chambon, A. Rivaton, J. L. Gardette, S. Guillerez and N. Lemaître, *Sol. Energy Mater. Sol. Cells*, 2010, **94**, 1572–1577.

139 R. A. Street, J. E. Northrup and B. S. Krusor, *Phys. Rev. B: Condens. Matter Mater. Phys.*, 2012, **85**, 205211.

140 A. Tournebize, P. O. Bussière, P. Wong-Wah-Chung, S. Thérias, A. Rivaton, J. L. Gardette, S. Beaupré and M. Leclerc, *Adv. Energy Mater.*, 2013, **3**, 478–487.

141 R. A. Street, Y. Yang, B. C. Thompson and I. McCulloch, *J. Phys. Chem. C*, 2016, **120**, 22169–22178.

142 N. Sai, K. Leung, J. Zador and G. Henkelman, *Phys. Chem. Chem. Phys.*, 2014, **16**, 8092–8099.

143 I. V. Martynov, L. N. Inasaridze and P. A. Troshin, *ChemSusChem*, 2022, **15**, e202101336.

144 A. Tournebize, J.-L. Gardette, C. Taviot-Guého, D. Bégué, M. A. Arnaud, C. Dagron-Lartigau, H. Medlej, R. C. Hiorns, S. Beaupré, M. Leclerc and A. Rivaton, *Polym. Degrad. Stab.*, 2015, **112**, 175–184.

145 A. Tournebize, I. F. Domínguez, G. E. Morse, C. Taviot-Guého, A. Rivaton, H. Peisert and T. Chassé, *Polym. Degrad. Stab.*, 2017, **146**, 155–160.

146 M. A. Anderson, A. Hamstra, B. W. Larson and E. L. Ratcliff, *J. Mater. Chem. A*, 2023, **11**, 17858–17871.

147 P. M. Kuznetsov, I. V. Martynov, I. S. Zhidkov, L. G. Gutsev, E. A. Komissarova, A. V. Maskaev, A. I. Kukharenko, F. A. Prudnov and P. A. Troshin, *J. Phys. Chem. B*, 2023, **127**, 6432–6439.

148 D. E. Shen, A. W. Lang, G. S. Collier, A. M. Österholm, E. M. Smith, A. L. Tomlinson and J. R. Reynolds, *Chem. Mater.*, 2022, **34**, 1041–1051.

149 K. O. Brinkmann, T. Becker, F. Zimmermann, C. Kreusel, T. Gahlmann, M. Theisen, T. Haeger, S. Olthof, C. Tuckmantel, M. Gunster, T. Maschwitz, F. Gobelsmann, C. Koch, D. Hertel, P. Caprioglio, F. Pena-Camargo, L. Perdigon-Toro, A. Al-Ashouri, L. Merten, A. Hinderhofer, L. Gomell, S. Zhang, F. Schreiber, S. Albrecht, K. Meerholz, D. Neher, M. Stolterfoht and T. Riedl, *Nature*, 2022, **604**, 280–286.

150 H. Gao, Y. Sun, L. Meng, C. Han, X. Wan and Y. Chen, *Small*, 2023, **19**, e2205594.

151 W. R. Xu, Y. L. Chang, X. W. Zhu, Z. H. Wei, X. L. Zhang, X. N. Sun, K. Lu and Z. X. Wei, *Chin. Chem. Lett.*, 2022, **33**, 123–132.

152 C. Y. Xu, Z. J. Zhao, K. X. Yang, L. B. Niu, X. L. Ma, Z. J. Zhou, X. L. Zhang and F. J. Zhang, *J. Mater. Chem. A*, 2022, **10**, 6291–6329.

153 Z. Zhang, Y. Wang, C. Sun, Z. Liu, H. Wang, L. Xue and Z. G. Zhang, *Nano Select*, 2021, **3**, 233–247.

154 H. Tang, C. Q. Yan, J. M. Huang, Z. P. Kan, Z. Y. Xiao, K. Sun, G. Li and S. R. Lu, *Matter*, 2020, **3**, 1403–1432.

155 Y. Lin, Y. Li and X. Zhan, *Chem. Soc. Rev.*, 2012, **41**, 4245–4272.

156 X. Sun, J. Lv, C. Zhang, K. Wang, C. Yang, H. Hu and X. Ouyang, *Sol. RRL*, 2023, **7**, 2300332.

157 H. Tang, C. Yan, J. Huang, Z. Kan, Z. Xiao, K. Sun, G. Li and S. Lu, *Matter*, 2020, **3**, 1403–1432.

158 C. Xu, Z. Zhao, K. Yang, L. Niu, X. Ma, Z. Zhou, X. Zhang and F. Zhang, *J. Mater. Chem. A*, 2022, **10**, 6291–6329.

159 Y. Sun, L. Nian, Y. Kan, Y. Ren, Z. Chen, L. Zhu, M. Zhang, H. Yin, H. Xu, J. Li, X. Hao, F. Liu, K. Gao and Y. Li, *Joule*, 2022, **6**, 2835–2848.

160 Y. Gao, X. Yang, R. Sun, L.-Y. Xu, Z. Chen, M. Zhang, H. Zhu and J. Min, *Joule*, 2023, **7**, 2845–2858.

161 B. Kan, M. Li, Q. Zhang, F. Liu, X. Wan, Y. Wang, W. Ni, G. Long, X. Yang, H. Feng, Y. Zuo, M. Zhang, F. Huang, Y. Cao, T. P. Russell and Y. Chen, *J. Am. Chem. Soc.*, 2015, **137**, 3886–3893.

162 W. Xu, Y. Chang, X. Zhu, Z. Wei, X. Zhang, X. Sun, K. Lu and Z. Wei, *Chin. Chem. Lett.*, 2022, **33**, 123–132.

163 A. B. Tamayo, X.-D. Dang, B. Walker, J. Seo, T. Kent and T.-Q. Nguyen, *Appl. Phys. Lett.*, 2009, **94**, 103301.

164 B. Walker, A. B. Tamayo, X. D. Dang, P. Zalar, J. H. Seo, A. Garcia, M. Tantiwiwat and T. Q. Nguyen, *Adv. Funct. Mater.*, 2009, **19**, 3063–3069.

165 R. Sun, Y. Wu, J. Guo, Y. H. Wang, F. Qin, B. X. Shen, D. H. Li, T. Wang, Y. W. Li, Y. H. Zhou, G. H. Lu, Y. F. Li and J. Min, *Energy Environ. Sci.*, 2021, **14**, 3174–3183.

166 R. Cheacharoen, W. R. Mateker, Q. Zhang, B. Kan, D. Sarkisian, X. F. Liu, J. A. Love, X. J. Wan, Y. S. Chen, T. Q. Nguyen, G. C. Bazan and M. D. McGehee, *Sol. Energy Mater. Sol. Cells*, 2017, **161**, 368–376.

167 K. K. Zhou, K. H. Xian and L. Ye, *InfoMat*, 2022, **4**, e12270.

7452 | *Chem. Soc. Rev.*, 2024, **53**, 7426–7454

This journal is © The Royal Society of Chemistry 2024

168 M. Kataria, H. D. Chau, N. Y. Kwon, S. H. Park, M. J. Cho and D. H. Choi, *ACS Energy Lett.*, 2022, **7**, 3835–3854.

169 A. Facchetti, *Mater. Today*, 2013, **16**, 123–132.

170 T. Yang and C. L. Zhan, *Sci. China: Chem.*, 2023, **66**, 2513–2531.

171 Z. Wang, X. Wang, L. Tu, H. Wang, M. Du, T. Dai, Q. Guo, Y. Shi and E. Zhou, *Angew. Chem., Int. Ed.*, 2024, e202319755.

172 B. Liu, W. Xu, R. Ma, J. W. Lee, T. A. Dela Pena, W. Yang, B. Li, M. Li, J. Wu, Y. Wang, C. Zhang, J. Yang, J. Wang, S. Ning, Z. Wang, J. Li, H. Wang, G. Li, B. J. Kim, L. Niu, X. Guo and H. Sun, *Adv. Mater.*, 2023, **35**, e2308334.

173 R. Sun, W. Wang, H. Yu, Z. Chen, X. Xia, H. Shen, J. Guo, M. Shi, Y. Zheng, Y. Wu, W. Yang, T. Wang, Q. Wu, Y. Yang, X. Lu, J. Xia, C. J. Brabec, H. Yan, Y. Li and J. Min, *Joule*, 2021, **5**, 1548–1565.

174 W. Y. Yang, W. Wang, Y. H. Wang, R. Sun, J. Guo, H. N. Li, M. M. Shi, J. Guo, Y. Wu, T. Wang, G. H. Lu, C. J. Brabec, Y. F. Li and J. Min, *Joule*, 2021, **5**, 1209–1230.

175 J. L. Song, L. L. Ye, C. H. Liu, Y. H. Cai, C. Zhang, G. C. Yue, Y. Li, M. H. Jee, Y. Zhao, D. H. Wei, H. Y. Woo and Y. M. Sun, *Energy Environ. Sci.*, 2023, **16**, 5371–5380.

176 J. Guo, T. Wang, Y. Wu, R. Sun, Q. Wu, W. Wang, H. Wang, X. Xia, X. Lu, T. Wang and J. Min, *J. Mater. Chem. C*, 2022, **10**, 1246–1258.

177 Q. Wu, W. Wang, Z. Chen, X. Xia, M. Gao, H. Shen, H. Zhu, X. Lu, L. Ye, J. Xia and J. Min, *J. Mater. Chem. C*, 2022, **10**, 1850–1861.

178 S. Liang, C. Xiao, C. Xie, B. Liu, H. Fang and W. Li, *Adv. Mater.*, 2023, **35**, e2300629.

179 J. Guo, Y. Wu, W. Wang, T. Wang and J. Min, *Sol. RRL*, 2022, **6**, 2101024.

180 X. Yang, M. Chen, S. Wang, Y. Gao, Y. Shao, L.-Y. Xu, Y. Wu, Y. Wang, R. S. Ashraf, S. Ponomarenko, Y. Luponosov and J. Min, *Giant*, 2023, **16**, 100191.

181 S. Liang, X. Jiang, C. Xiao, C. Li, Q. Chen and W. Li, *Acc. Chem. Res.*, 2021, **54**, 2227–2237.

182 S. Liang, J. Wang, Y. Ouyang, W. L. Tan, C. R. McNeill, Q. Chen, Z. Tang and W. Li, *Macromolecules*, 2022, **55**, 2517–2523.

183 D. Xia, S. Zhou, W. L. Tan, S. Karuthedath, C. Xiao, C. Zhao, F. Laquai, C. R. McNeill and W. Li, *Aggregate*, 2022, **4**, e279.

184 Y. K. He, N. Li, T. Heumüller, J. Wortmann, B. Hanisch, A. Aubele, S. Lucas, G. T. Feng, X. D. Jiang, W. W. Li, P. Bäuerle and C. J. Brabec, *Joule*, 2022, **6**, 1160–1171.

185 W. Wei, Y. Gao, Y. Wu, X. Yang, Z. Chen, Z. Chen, T. Wang, R. Sun, Q. Wu, X. Hao, H. Zhu, S. Ponomarenko, Y. Luponosov and J. Min, *J. Mater. Chem. A*, 2022, **10**, 18753–18761.

186 Y. Gao, B. Xiao, S. Wang, M. Chen, W. Wang, X. Yang, Y. Shao, R. Sun and J. Min, *Sci. China: Chem.*, 2023, **66**, 3205–3212.

187 X. Yang, Y. Wu, Y. Gao, J. Guo, W. Wang and J. Min, *Adv. Funct. Mater.*, 2022, **33**, 2208412.

188 Y. Cheng, Q. Mao, C. Zhou, X. Huang, J. Liu, J. Deng, Z. Sun, S. Jeong, Y. Cho, Y. Zhang, B. Huang, F. Wu, C. Yang and L. Chen, *Angew. Chem., Int. Ed.*, 2023, **62**, e202308267.

189 Y. He, N. Li and C. J. Brabec, *Org. Mater.*, 2021, **03**, 228–244.

190 J. Roncali, *Adv. Energy Mater.*, 2021, **11**, 2102987.

191 B. Li, X. Yang, S. Li and J. Yuan, *Energy Environ. Sci.*, 2023, **16**, 723–744.

192 Y. Cheng, B. Huang, Q. Mao, X. Huang, J. Liu, C. Zhou, W. Zhou, X. Ren, S. Kim, W. Kim, Z. Sun, F. Wu, C. Yang and L. Chen, *Adv. Mater.*, 2024, e2312938.

193 Y. He, B. Wang, L. Lüer, G. Feng, A. Osvet, T. Heumüller, C. Liu, W. Li, D. M. Guldi, N. Li and C. J. Brabec, *Adv. Energy Mater.*, 2021, **12**, 2103406.

194 Y. Wu, J. Guo, W. Wang, Z. Chen, Z. Chen, R. Sun, Q. Wu, T. Wang, X. Hao, H. Zhu and J. Min, *Joule*, 2021, **5**, 1800–1815.

195 I. E. Jacobs, F. Wang, Z. I. B. Valdez, A. N. A. Oviedo, D. J. Bilsky and A. J. Moulé, *J. Mater. Chem. C*, 2018, **6**, 219–225.

196 A. Classen, T. Heumueller, I. Wabra, J. Gerner, Y. K. He, L. Einsiedler, N. Li, G. J. Matt, A. Osvet, X. Y. Du, A. Hirsch and C. J. Brabec, *Adv. Energy Mater.*, 2019, **9**, 1902124.

197 X. Xu, J. Xiao, G. Zhang, L. Wei, X. Jiao, H. L. Yip and Y. Cao, *Sci. Bull.*, 2020, **65**, 208–216.

198 D. Yang, F. C. Löhrer, V. Körstgens, A. Schreiber, S. Bernstorff, J. M. Buriak and P. Müller-Buschbaum, *ACS Energy Lett.*, 2019, **4**, 464–470.

199 H. T. Liu, Y. B. Li, S. H. Xu, Y. H. Zhou and Z. A. Li, *Adv. Funct. Mater.*, 2021, **31**, 2106735.

200 F. Qin, W. Wang, L. Sun, X. Jiang, L. Hu, S. Xiong, T. Liu, X. Dong, J. Li, Y. Jiang, J. Hou, K. Fukuda, T. Someya and Y. Zhou, *Nat. Commun.*, 2020, **11**, 4508.

201 B. W. Xu and J. H. Hou, *Adv. Energy Mater.*, 2018, **8**, 1800022.

202 D. Baran, N. Gasparini, A. Wadsworth, C. H. Tan, N. Wehbe, X. Song, Z. Hamid, W. Zhang, M. Neophytou, T. Kirchartz, C. J. Brabec, J. R. Durrant and I. McCulloch, *Nat. Commun.*, 2018, **9**, 2059.

203 F. Qin, L. Sun, H. Chen, Y. Liu, X. Lu, W. Wang, T. Liu, X. Dong, P. Jiang, Y. Jiang, L. Wang and Y. Zhou, *Adv. Mater.*, 2021, **33**, e2103017.

204 L. Hu, Y. Liu, L. Mao, S. X. Xiong, L. L. Sun, N. Zhao, F. Qin, Y. Y. Jiang and Y. H. Zhou, *J. Mater. Chem. A*, 2018, **6**, 2273–2278.

205 W. Zeng, X. Zhou, B. Du, L. Hu, C. Xie, W. Wang, Y. Jiang, T. Wang and Y. Zhou, *Adv. Energy Sustainability Res.*, 2021, **2**, 2000094.

206 A. Prasetio, M. Jahandar, S. Kim, J. Heo, Y. H. Kim and D. C. Lim, *Adv. Sci.*, 2021, **8**, 2100865.

207 Z. Q. Zhang, Z. L. Zhang, Y. F. Yu, B. Zhao, S. Li, J. Zhang and S. T. Tan, *J. Energy Chem.*, 2020, **47**, 196–202.

208 Y. Li, T. Li, J. Wang, X. Zhan and Y. Lin, *Sci. Bull.*, 2022, **67**, 171–177.

This journal is © The Royal Society of Chemistry 2024

Chem. Soc. Rev., 2024, **53**, 7426–7454 | **7453**

209 M. Kyeong, J. Lee, M. Daboczi, K. Stewart, H. F. Yao, H. J. Cha, J. Luke, K. Lee, J. R. Durrant, J. S. Kim and S. Hong, *J. Mater. Chem. A*, 2021, **9**, 13506–13514.

210 S. Xiong, L. Hu, L. Hu, L. Sun, F. Qin, X. Liu, M. Fahlman and Y. Zhou, *Adv. Mater.*, 2019, **31**, e1806616.

211 X. Y. Zhu, L. Hu, W. Wang, X. S. Jiang, L. Hu and Y. H. Zhou, *ACS Appl. Energy Mater.*, 2019, **2**, 7602–7608.

212 Y. P. Qin, N. Balar, Z. X. Peng, A. Gadisa, I. Angunawela, A. Bagui, S. Kashani, J. H. Hou and H. Ade, *Joule*, 2021, **5**, 2129–2147.

213 S. H. K. Paleti, S. Hultmark, J. Han, Y. Wen, H. Xu, S. Chen, E. Jarsvall, I. Jalan, D. R. Villalva, A. Sharma, J. I. Khan, E. Moons, R. Li, L. Yu, J. Gorenflot, F. Laquai, C. Muller and D. Baran, *Nat. Commun.*, 2023, **14**, 4608.

214 J. Xiao, N. Li, Q. Yin, Y. Min and H. L. Yip, *Adv. Opt. Mater.*, 2024, **12**, 2302202.

215 Z. Xing, X. Wu, T. Chen, S. Ye, S. Wang, Y. Pan, S. Li, M. Shi and H. Chen, *J. Mater. Chem. A*, 2024, **12**, 11286–11294.

216 X. Y. Jiang, A. J. Gillett, T. L. Zheng, X. Song, J. E. Heger, K. Sun, L. V. Spanier, R. J. Guo, S. Z. Liang, S. Bernstorff and P. Müller-Buschbaum, *Energy Environ. Sci.*, 2023, **16**, 5970–5981.

217 D. F. Zhang, C. Liu, K. C. Zhang, Y. H. Jia, W. K. Zhong, W. D. Qiu, Y. F. Li, T. Heumueller, K. Forberich, V. M. Le Corre, L. Lüer, N. Li, F. Huang, C. J. Brabec and L. Ying, *Energy Environ. Sci.*, 2023, **16**, 5970–5981.

218 Y. Li, X. Huang, A. R. Mencke, S. K. Kandappa, T. Wang, K. Ding, Z. Q. Jiang, A. Amassian, L. S. Liao, M. E. Thompson and S. R. Forrest, *Proc. Natl. Acad. Sci. U. S. A.*, 2023, **120**, e2301118120.

219 J. Y. Xiao, M. R. Ren, G. C. Zhang, J. B. Wang, D. L. Zhang, L. L. Liu, N. Li, C. J. Brabec, H. L. Yip and Y. Cao, *Sol. RRL*, 2019, **3**, 1900077.

220 N. Gasparini, H. K. Paleti, J. Bertrandie, G. L. Cai, G. C. Zhang, A. Wadsworth, X. H. Lu, H. L. Yip, I. McCulloch and D. Baran, *ACS Energy Lett.*, 2020, **5**, 1371–1379.

221 S. H. K. Paleti, S. Hultmark, N. Ramos, N. Gasparini, A. H. Emwas, J. Martin, C. Müller and D. Baran, *Sol. RRL*, 2022, **6**, 2200436.

222 Y. J. Cui, Z. Chen, P. P. Zhu, W. Ma, H. M. Zhu, X. F. Liao and Y. W. Chen, *Sci. China: Chem.*, 2023, **66**, 1179–1189.

223 M. Salvador, N. Gasparini, J. D. Perea, H. Paleti, A. Distler, L. N. Inasaridze, P. A. Troshin, L. Lüer, H. J. Egelhaaf and C. Brabec, *Energy Environ. Sci.*, 2017, **10**, 2005–2016.

224 A. Karki, A. J. Gillett, R. H. Friend and T. Q. Nguyen, *Adv. Energy Mater.*, 2020, **11**, 2003441.

225 Q. Burlingame, M. Ball and Y. L. Loo, *Nat. Energy*, 2020, **5**, 947–949.

7454 | *Chem. Soc. Rev.*, 2024, **53**, 7426–7454

This journal is © The Royal Society of Chemistry 2024